Design and Characterization of Photonic Crystal Fiber for Broadband Dispersion Compensation

by

(Md. Mejbaul Haque)

A thesis submitted in partial fulfillment of the requirements for the degree of
Master of Science in Electrical and Electronic Engineering

Khulna University of Engineering & Technology
Khulna 9203, Bangladesh

October 2013

Declaration

This is to certify that the thesis work entitled "Design and Characterization of Photonic Crystal Fiber for Broadband Dispersion Compensation" has been carried out by Md. Mejbaul Haque in the Department of Electrical and Electronic Engineering, Khulna University of Engineering & Technology, Khulna, Bangladesh. The above thesis work or any part of this work has not been submitted anywhere for the award of any degree or diploma.

H S Palma

Signature of Supervisor

Signature of Candidate

Approval

This is to certify that the thesis work submitted by Md. Mejbaul Haque entitled "Design and Characterization of Photonic Crystal Fiber for Broadband Dispersion Compensation" has been approved by the board of examiners for the partial fulfillment of the requirements for the degree of *Master of Science in Electrical and Electronic Engineering* from the Department of Electrical and Electronic Engineering, Khulna University of Engineering & Technology, Khulna, Bangladesh in October 2013.

BOARD OF EXAMINERS

1. _____ 31.10.13
   Dr. Mohammad Shaifur Rahman
   Professor
   Department of Electrical and Electronic Engineering
   Khulna University of Engineering & Technology
   — Chairman (Supervisor)

2. _____ 31.10.2013
   Head of the Department
   Department of Electrical and Electronic Engineering
   Khulna University of Engineering & Technology
   — Member

3. _____ 31.10.13
   Dr. Md. Rafiqul Islam
   Professor
   Department of Electrical and Electronic Engineering
   Khulna University of Engineering & Technology
   — Member

4. _____ 31.10.13
   Dr. Md. Shahjahan
   Professor
   Department of Electrical and Electronic Engineering
   Khulna University of Engineering & Technology
   — Member

5. _____ 31.10.2013
   Dr. S. M. Abdur Razzak
   Professor
   Department of Electrical and Electronic Engineering
   Rajshahi University of Engineering & Technology
   — Member (External)

Abstract

In long range optical fiber communication, dispersion is a major technological challenge that causes broadening of optical pulses when transmitted through the fiber. As a result, it limits the maximum transmission distance and the bit rate. Many efforts have been drawn to the development of dispersion compensating techniques to mitigate the effect of pulse broadening. In this thesis, modeling and analysis of broadband dispersion compensating photonic crystal fibers (DC-PCFs) for dispersion compensation of standard single mode fibers (SMFs) have been carried out. Three different PCF models such as circular photonic crystal fiber (C-PCF), modified circular photonic crystal fiber (M-CPCF) and modified octagonal photonic crystal fiber (M-OPCF) have been designed and their guiding properties have been analyzed using finite element method (FEM). A perfectly matched layer (PML) circular boundary is has been used to calculate the confinement loss. The proposed C-PCF exhibits a high negative dispersion coefficient of about -248.65 to -1069 ps/(nm.km) over the wavelength ranging from 1340 to 1640 nm. It is also demonstrated that the proposed C-PCF shows an effective dispersion of about ± 0.8 ps/(nm.km) over the band from 1400 nm to 1610 nm and. However, birefringence of C-PCF is not found so high and particularly in the order of about 7×10^{-4} at 1550 nm wavelength. On the other hand, M-CPCF shows a high negative dispersion coefficient of -203.8 to -835.14 ps/(nm.km) over 1340 to 1640 nm wavelength with a high birefringence of 2.2×10^{-2} at 1550 nm wavelength. In addition, the effective dispersion is found less than ± 0.8 ps/(nm.km) over the band from 1400 to 1640 nm. Finally, M-OPCF achieves negative dispersion coefficient of about -276.27 to -889.21 ps/(nm.km) over 1340 nm to 1640 nm with a high birefringence of 2.53×10^{-2} at 1550 nm wavelength. Moreover, the effective dispersion is less than ± 0.8 ps/(nm.km) over the band from 1430 to 1610 nm wavelength. Furthermore, the dispersion slope of the proposed DC-PCFs have been determined and found negative over the band of interest and residual dispersion slope (RDS) of the proposed DC –PCFs is achieved equal to that of conventional SMFs of about 0.0036 nm^{-1} at 1550 nm wavelength. In addition to these, effective area, confinement losses, and dispersion behavior for fiber's global diameter variations and fiber's structural parameters variation have been investigated. It has been found that the structural parameters and also global diameter variations do not affect the dispersion accuracy of the proposed DC-PCFs.

Acknowledgement

I would like to gratefully acknowledge the enthusiastic supervision of Dr. Mohammad Shaifur Rahman during this work. His understanding, encouragement, motivation and expert guidance have provided a good basis for my entire research work. I am grateful to him and expressing my sincere gratitude and thanks for having given me the opportunity to do research.

I would also like to thank Dr. S. M. Abdur Razzak, Department of Electrical and Electronic Engineering, Rajshahi University of Engineering & Technology and all members of his research group, for giving me valuable suggestions throughout my research. I extend my sincere gratitude and appreciation to Dr. Md. Rafiqul Islam (1), Dr. Mohiuddin Ahmad, Dr. Md. Rafiqul Islam (2) and Mr. Md. Sherajul Islam who had been my course teachers during my graduate studies. I am indebted to all my faculty colleagues for their kind cooperation and providing me an excellent work environment during the past years.

I feel a deep sense of gratitude to my parents who formed part of my vision and taught me the good things that really matter in life. Last but not the least, I would like to record that this work would be well-nigh impossible to complete without the inspiration from my parents and my wife Mst. Sabrina Haque as they give continuous support and encouragement throughout the research. Finally, my profound thanks go to the chairman and the members of the dissertation committee for their valuable comments which were supportive in enriching the quality of my thesis.

Author

Contents

Abstract i
Acknowledgement ii
List of Figures v
List of Tables ix

1. Introduction
1.1 Background 1
1.2 Motivation 2
1.3 Literature review 3
1.4 Light spectrum and telecommunication band 4
1.5 Objectives of the thesis 6
1.6 Thesis outline 6
1.7 Summary 7

2. Fundamentals of Photonic Crystal Fiber
2.1 Introduction 10
2.2 Construction of PCF 10
2.3 Classification of different PCF 12
2.3.1 Highly nonlinear (HNL) fiber 12
2.3.2 Large mode area (LMA) fiber 12
2.3.3 Hole assisted PCF (HA-PCF) 12
2.3.4 High numerical aperture (HNA) fiber 12
2.4 Light guiding mechanism of PCF 1
2.5 Difference between PCF and conventional fiber 14
2.6 Guiding properties of the PCF 15
2.6.1 Chromatic dispersion 15
2.6.2 Birefringence 16
2.6.3 Confinement loss 16
2.6.4 Mode field diameter and effective area 17
2.6.5 Single mode or multimode response 18
2.7 Applications of PCF 18
2.8 Conclusion 18

3. Numerical Modeling and Analysis of DC-PCFs
3.1 Introduction 21
3.2 Existing numerical methods 21
3.3 Formulation of FEM method 22
3.4 Determination of modal properties of PCF 23

3.4.1 Chromatic dispersion..... 23
3.4.2 Dispersion slope and RDS..... 24
3.4.3 Effective dispersion..... 24
3.4.4 Confinement loss..... 24
3.4.5 Birefringence..... 25
3.4.6 Effective area..... 25
3.4.7 Single and multimode response..... 25
3.5 Conclusion..... 26

4. Design and Characterization of Broadband DC-PCF
4.1 Introduction..... 29
4.2 Requirements for broadband dispersion and dispersion slope compensation... 29
4.3 Proposed DC-PCF models..... 30
4.3.1 Structure of C-PCF 30
4.3.2 Structure of M-CPCF 32
4.3.3 Structure of M-OPCF 24
4.4 Numerical simulation using COMSOL Multiphysics 4.2 34
4.4.1 Simulation results of C-PCF 35
4.4.2 Simulation results of M-CPCF..... 43
4.4.3 Simulation results of M-OPCF..... 50
4.5 Comparison between proposed DC-PCFs and some other DC-PCFs 59
4.6 Conclusion..... 61

5. Conclusions and Suggestions
5.1 Conclusion..... 64
5.2 Suggestions for future works..... 66

List of Figures

1.1	Electromagnetic spectrum.	5
1.2	Optical attenuation characteristics of silica fiber and the telecom windows.	6
2.1	Schematic cross sections and index-profiles of (a) IG-PCF (the dotted circle in the center indicates an omitted air-hole) and (b) HC or PBG PCF (the larger circle in the center represents the hollow core).	11
2.2	Types of PCFs (a) PM-PCF, (b) HA-PCF, (c) HNA-PCF, and (d) Bragg Fiber.	13
2.3	Schematic cross sections and index-profiles of (a) PCFs (a missing air-hole in the center represents the core) and (b) Ordinary fibers.	14
2.4	Dispersion phenomena in an optical fiber.	15
2.5	Confinement losses in index-guiding PCF.	17
2.6	Gaussian intensity distribution in a single-mode optical fiber.	17
4.1	Structure of the proposed C-PCF for broadband dispersion compensation.	31
4.2	Structure of the proposed M-CPCF for broadband dispersion compensation.	33
4.3	Structure of the proposed O-PCF for broadband dispersion compensation.	33
4.4	Dispersion properties of C-PCF for fiber's global diameter variation.	35
4.5	Dispersion properties of C-PCF: optimum dispersion and effects of changing pitch keeping all d/Λ constant.	36
4.6	Dispersion properties of C-PCF: optimum dispersion and effects of changing d_1.	36
4.7	Dispersion properties of C-PCF: optimum dispersion and effects of changing d_2.	37
4.8	Dispersion properties of C-PCF: optimum dispersion and effects of changing d_4.	37
4.9	Effect of changing pitch, Λ on residual dispersion slope.	38
4.10	Dispersion slope of C-PCF showing the effects of changing Λ.	38
4.11	Variation of effective dispersion against wavelength of 818.4 m long optimized C-PCF to compensate for a 40 km long standard SMFs.	39
4.12	Birefringence property of the proposed C-PCF for the optimum design parameters: $\Lambda=1.0$, $d_1/\Lambda=0.95$, $d_2/\Lambda=0.81$, $d_3/\Lambda=0.98$, $d_4/\Lambda=0.60$.	39
4.13	Wavelength response of chromatic dispersion of the proposed C-PCF for both	40

x- and y-polarization for the optimum design parameters.

4.14 Variation in the effective refractive index for both x- and y-polarization for the optimized C-PCF. 40

4.15 Effective area of the proposed C-PCF for optimum design parameters and also for fiber's global diameter variations of order ±1 to ±2% around the optimum value. 41

4.16 Confinement loss of the proposed C-PCF for the optimum parameters and also showing the effect of increasing number of rings confinement loss. 41

4.17 Variation of effective V-parameter for the optimized C-PCF. 42

4.18 Dispersion properties of M-CPCF for fiber's global diameter variation. 43

4.19 Dispersion properties of M-CPCF: optimum dispersion and effects of changing pitch keeping all d/Λ constant. 44

4.20 Dispersion properties of M-CPCF: optimum dispersion and effects of tuning, d_1. 44

4.21 Dispersion properties of M-CPCF: optimum dispersion and effects of tuning, d_2. 45

4.22 Dispersion properties of M-CPCF: optimum dispersion and effects of tuning, d_3. 45

4.23 Effect of pitch, Λ on residual dispersion slope of the proposed M-CPCF. 46

4.24 Dispersion slope of M-CPCF showing the effects of Λ. 46

4.25 Variation of effective dispersion against wavelength of 1.15 km long optimized M-CPCF to compensate for a 40 km long standard SMFs. 47

4.26 Birefringence property of the proposed M-CPCF for the optimum design parameters: $\Lambda=1.0$, $d_1/\Lambda=0.95$, $d_2/\Lambda=0.70$, $d_3/\Lambda=0.60$, $\eta=0.22$. 47

4.27 Wavelength dependent response of effective refractive index of the proposed M-CPCF for both x- and y-polarization for the optimum design parameters. 48

4.28 Wavelength response of chromatic dispersion of the proposed C-PCF for both x- and y-polarization for the optimum design parameters. 48

4.29 Effective area of the proposed M-CPCF for optimum design parameters and also for fiber's global diameter variations of order ±1 to ±2% around the optimum value. 49

4.30 Confinement loss of the proposed M-CPCF for the optimum parameters and 49

also for fiber's global diameter variations of order ±1 to ±2% around the optimum value.

4.31 Variation of effective V-parameter for the optimized M-CPCF. 50

4.32 Dispersion properties of M-OPCF: optimum dispersion and dispersion due to fiber's global diameter variation. 51

4.33 Dispersion properties of M-OPCF: optimum dispersion and effects of changing pitch Λ keeping all d/Λ constant. 51

4.34 Dispersion properties of M-OPCF: optimum dispersion and effects of tuning, d_1. 52

4.35 Dispersion properties of M-OPCF: optimum dispersion and effects of tuning, d_2. 52

4.36 Dispersion properties of M-OPCF: optimum dispersion and effects of tuning, d_3. 53

4.37 Effect of pitch, Λ on residual dispersion slope of the proposed M-OPCF. 53

4.38 Effect of pitch, Λ on dispersion slope of the proposed M-OPCF. 54

4.39 Variation of effective dispersion against wavelength of 1.10 km long optimized M-OPCF to compensate for a 40 km long standard SMFs. 54

4.40 Birefringence property of the proposed M-OPCF for the optimum design parameters: $d_1/\Lambda = 0.73$, $d_2/\Lambda = 0.53$, $d_3/\Lambda = 0.70$, and $\eta = 0.307$. 55

4.41 Wavelength dependent response of effective refractive index of the proposed M-OPCF for both x- and y-polarization for the optimum design parameters. 55

4.42 Wavelength response of chromatic dispersion of the proposed M-OPCF for both x- and y-polarization for the optimum design parameters. 56

4.43 Effective area of the proposed M-OPCF for optimum design parameters and also for fiber's global diameter variations of order ±1 to ±2% around the optimum value. 57

4.44 Confinement loss of the proposed M-OPCF for the optimum parameters and also for fiber's global diameter variations of order ±1 to ±2% around the optimum value. 58

4.45 Variation of effective V-parameter for the optimized M-OPCF. 58

4.46 Comparison between relative dispersion slope for the proposed DC-PCFs. 60

4.47 Comparison between effective dispersion of the proposed DC-PCFs. 60
4.48 Comparison between confinement losses of the proposed DC-PCFs. 61

List of Tables

1	Electromagnetic band	5
2	Configuration of notebook	35
3	Comparison between properties of the proposed DC-PCFs and other DC-PCFs at 1550 nm wavelength	59

CHAPTER I

Introduction

1.1 Background

The invention of optical fiber is the most remarkable achievement in the history of telecommunication which has gradually replaced copper wire in telecommunication systems because of its many unique and attractive features [1]. Communication system employing optical fiber as a transmission link permits signal transmission over longer distances and improves rates. Moreover, optical fiber is also being used in non-telecommunication systems such as remote sensing, medical imaging, illuminations, machining, and welding applications because of its small size, light weight, chemically inertness, higher bandwidth, longer repeater span, electromagnetic immunity, and many other interesting properties [2]. Optical fiber is nothing but a waveguide that guides signals in the form of light. It is cylindrical in shape and typically constructed using two glasses which are prepared from the common material silica (SiO_2). However, it consists of a higher refractive index solid glass core surrounded by solid glass with a relatively lower refractive index than that of core which forms the homogeneous cladding [3]. The difference in refractive index is an important parameter that helps to trap the light inside the fiber core. The signal in the form of light is guided through the optical fiber core based on total internal reflection (TIR) mechanism [4]. This type of optical fiber is called conventional optical fiber. Though conventional optical fibers are used in both telecom and non-telecom applications, there is something that these fibers cannot do. As properties of the silica glass are not flexible, ordinary optical fibers cannot suit certain emerging applications because tailoring the properties of conventional optical fiber is very difficult. To overcome the limitations of conventional optical fibers, the invention of the photonic crystal fiber (PCF) which is also called the holey optical fiber (HOF) or microstructure optical fiber (MOF), has led to another potential breakthrough in fiber optics technology [5]. The PCF is a single material optical fiber which contains microscopic air-holes in a silica background running down the length of the fiber. As a result, the entire structure forms silica-air microstructure that causes lower refractive index in the cladding region and higher refractive index in the core [6]. The PCF can be divided into two categories depending on their internal construction. Air holes can be arranged in the cladding either in a periodic or an aperiodic fashion and air holes may be of any shape but circular or

elliptical are common. On the other hand, the core of PCF may be either solid or hollow and the light guiding mechanism within PCF completely depends on the construction of core. The PCF employing solid core guides optical signal in the form of light through the fiber based on the modified TIR mechanism like conventional optical fiber. In this case, the refractive index of the core is greater than the refractive index of the cladding. In contrast, the PCF with hollow core guides light based upon a very new mechanism which is called photonic band gap (PBG) where the refractive index of the core is less that the refractive index of the cladding [7]. Hence it is not mandatory that the core of PCF must be made of a higher refractive index material than the cladding as in the case of conventional optical fiber. Similarly, it is also not necessary that only the TIR mechanism confines light into the core of all optical fibers. PCF offers great flexibility in tailoring its properties with inclusions of tiny air-holes in the cladding and hence opens a wider design space [8]. In addition, the index contrast between the core and cladding increases due to the silica-air microstructure in the cladding which helps to tailor the optical properties of the PCF. Modulating some parameters of the silica-air microstructure, it is possible to tune the dispersion properties of the PCF which helps to specially design the broadband dispersion compensating fiber (DCF). In addition, it is possible to design application specific guiding properties by PCF which realizes a number of unusual and previously unimaginable properties like endlessly single mode operation [9], super high nonlinearities [10], very high or low birefringence [11], ultra-flattened and ultra-low chromatic dispersion [12], and many others. Hence, PCFs can easily outperform conventional fibers in many scientific and technological areas of applications for their superior and easy to tailor optical properties.

1.2 Motivation

The invention of PCF has opened up enormous scope for the optical fiber communication researchers to meet massive potential and promises. Hence, invention of the PCF is considered and recognized as a major breakthrough in fiber history [5]. The wide design space due to high index contrast, flexibility, superiority, and extraordinary optical properties are considered the key to numerous scientific and technological applications in both linear and nonlinear regimes [5, 13]. For example, medical sector requires lasers at new wavelengths or broadband light sources for diagnosis whereas the sensor industry is searching for environmental sensors. On the other hand, the telecommunication sector

looks for more efficient dispersion compensator, more flexible amplifiers, and low-cost fibers. PCF either hollow core or solid core indeed can serve as optical components for all these emerging sectors [14]. All these crucial tasks are great technological challenges to be solved. However, in long range optical fiber communication, broadening of optical pulses due to dispersion is a major technological challenge as it ultimately limits the maximum transmission distance and the bit rate when transmitted through the fiber [15]. Thus, the dispersion must be compensated in the long distance optical data transmission system to nullify the pulse broadening. Considering the massive potential of this growing field, this thesis is to contribute in designing more efficient broadband dispersion compensating fiber using PCF.

1.3 Literature review

After the first demonstration of the holey optical fiber in 1996 reported by Knight et al. [16], PCF research has been launched and from then, interest on this research field is increasing day by day due to its potential ability to exhibit some extraordinary optical properties which is not possible in conventional optical fiber. They have demonstrated practical realization of a holey fiber with periodic air-holes arranged in a hexagonal lattice [17] and discovered that holey fiber is similar to conventional fiber in the sense that light guiding mechanism in holey fiber is based on modified total internal reflection. However, significant differences between the conventional fibers and the PCFs are also observed in terms of design space and optical properties. In this thesis, focus will be given broadband dispersion compensation technique using PCF. Our aim is to design and characterize of PCFs for broadband dispersion compensation of single mode fiber (SMF) that will compensate both chromatic dispersion and polarization mode dispersion (PMD). It should be mentioned here that there are several dispersion management approaches such as soliton, fiber Bragg gratings, optical phase conjugation technique, Dispersion Compensating Fibers (DCFs) and so on. Among them, DCFs are widely used and commercially available tools for dispersion compensation which are designed to have large negative dispersion [18]. In order to reduce the length of DCF, we need high negative dispersion [19]. In addition, high negative dispersion of DCFs is needed to be achieved over a wide range of wavelength for Wavelength Division Multiplexing (WDM) transmissions [20]. Hence, compensation of dispersion and dispersion slope are simultaneously required. However, the major pitfall of conventional DCF is that it shows a

high negative dispersion peak only at a particular wavelength instead of a broad range [21]. So, the key issue is to achieve dispersion compensation over a wide band of wavelength. Recently, Photonic Crystal Fiber (PCF) which has gained attentions in many fields due to its novel properties such as controllable dispersion, birefringence, nonlinearity etc. and has become a promising candidate for addressing the issue of broadband dispersion compensation as it allows us to obtain relatively higher negative dispersion over a wide band of wavelength than that of conventional DCFs [22]. To compensate dispersion of Single Mode Fibers (SMFs), different types of PCF structures have already been proposed in [7-10]. PCF with hexagonal structure is proposed in [23] to compensate dispersion over 1460-1625 nm wavelength range but the negative dispersion is not sufficiently large and Relative Dispersion Slope (RDS) is not equal to SMF's RDS of 0.0036 nm^{-1} at 1.55 μm. M-OPCF has been studied in [24] which achieves negative dispersion of only -239.5 ps/(nm.km) at 1.55 μm with 90% slope matching. Although, high negative dispersion is achieved in [25] but available bandwidth for dispersion compensation is narrow and no effort was made to match RDS. PCF with dual concentric core without Ge doping have been proposed in [26] but insufficient bandwidth is further noticed. Recently, PCF for dispersion compensation of SMFs have been proposed in [21, 27] using five air-hole rings. However, PCF reported in [21] shows perfect RDS matching but exhibits insufficient negative dispersion of -130 to -360 ps/(nm.km) in a 1.30-1.60 μm wavelength range. In contrast, square-lattice PCF [27] reports a negative dispersion of -204.4 ps/(nm.km) and RDS of 0.003543 nm^{-1} at 1.55 μm wavelength. Moreover, high birefringence property is required to eliminate the effect of Polarization Mode Dispersion (PMD) but no attempt was made to eliminate PMD in their design. So, there is a still need for large negative dispersion and high birefringence over a wide range of wavelength with 100% slope matching.

1.4 Light spectrum and telecommunication band

The electromagnetic spectrum is the range of all possible frequencies of electromagnetic radiation. The visible light spectrum spreads from a 400 nm to 700 nm wavelength ranges, while optical fibers operate from the ultra-violet to the infrared region ranging from generally 300 to 1700 nm wavelengths. Telecommunication industries have been developed in the O band to L band (1.30 to 1.65 μm wavelength). Nowadays the 1.30 μm

window and 1.55 μm windows are in extensive use. Because of the high absorption losses around 1.40 μm wavelengths, this window is rarely used.

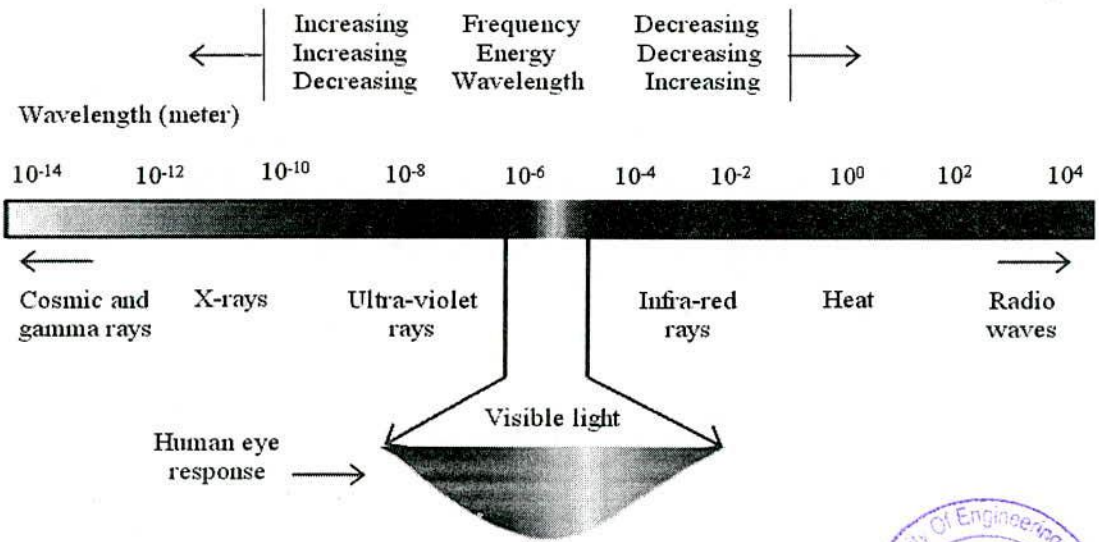

Fig. 1.1 Electromagnetic spectrum.

Table 1: Electromagnetic band

Band Name	Description	Range [nm]
O-band	Original	1260-1360
E-band	Extended	1360-1460
S-band	Short wavelength	1460-1530
C-band	Conventional	1530-1565
L-band	Long wavelength	1565-1625
U-band	Ultra-long wavelength	1625-1675

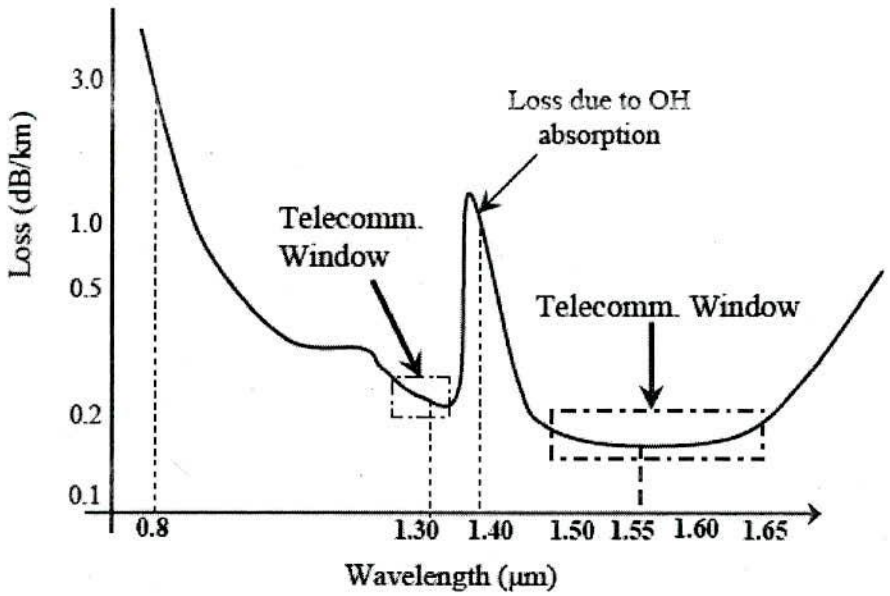

Fig. 1.2 Optical attenuation characteristics of silica fiber and the telecom windows.

1.5 Objectives of the thesis

The main objective of this research is to design a suitable PCF structure that can be used as DCF to address the dispersion compensation issues of SMFs in WDM applications. The proposed PCFs structures would be designed to meet the following requirements-

i. To obtain high negative dispersion over a wide range of wavelengths for compensating the chromatic dispersion of conventional optical fiber used in WDM system.
ii. To get RDS of the proposed PCFs equal to that of standard SMFs to ensure the slope matching.
iii. To minimize the effect of PMD by introducing high birefringence property in the proposed structures.
iv. To reduce the length of proposed PCFs by introducing high negative dispersion.
v. To investigate dispersion accuracy of the proposed PCFs considering fabrication tolerance.

1.6 Thesis outline

Chapter I covers general introduction of the thesis and Chapter II covers fundamental concepts of PCF in brief. Chapter III presents a brief discussion about the numerical computational methods for mode solutions of PCF and necessary equations to evaluate the light guiding properties of the designed PCF. Chapter IV presents scopes and constrains of

designing dispersion compensating PCF, an optimum dispersion compensating PCF design, its modal properties including dispersion, effective refractive index, effective dispersion, relative dispersion slope and birefringence, potential applications. Hence, Chapter IV also includes a comparison of properties between the designed PCFs and other similar PCFs in the peer reviewed literature. Finally, Chapter V includes conclusion and scopes for further study.

1.7 Summary

The general background PCF research field, factors influencing widespread applicability of these fibers, thesis motivation, literature review, light spectrum and telecom band, objectives and organization of the thesis has been presented in brief.

References

[1] S. V. Kartalopoulos, "DWDM Networks, Devices and Technology," John Wiley & Sons Inc., USA, 2003.

[2] J. Hecht, "Understanding Fiber Optics," Prentice Hall, USA, 3rd Edition, 1999.

[3] G. P. Agrawal, "Nonlinear Fiber Optics," Academic Press, USA, 2nd Edition, 1995.

[4] G. P. Agrawal, "Fiber-Optic Communication Systems," John Wiley & Sons Inc., USA, 3rd Edition, 2002.

[5] A. Bjarklev, J. Broeng, and A. S. Bjarklev, "Photonic Crystal Fibers," Kulawer Academic Press, USA, 2003.

[6] J. Broeng, D. Mogilevstev, S. E. Barkou, and A. Bjarklev, "Photonic crystal fibers: A new class of optical waveguides," *Optical Fiber Technology*, vol. 5, pp. 305–330, 1999.

[7] J. C. Knight, "Photonic crystal fibers," *Nature*, vol. 424, pp. 847-851, Aug. 2003.

[8] L. P. Shen, W. P. Hung, and S. S. Jian, "Design and optimization of photonic crystal fibers for broadband dispersion compensation," *IEEE Photonics Technology Letters*, vol. 15, no. 4, pp. 540-542, Apr. 2003.

[9] T. A. Birks, J. C. Knight, and P. St. J. Russell, "Endlessly single-mode photonic crystal fiber," *Optics Letters*, vol. 22, no. 13, pp. 961-963, July 1997.

[10] P. Petropoulus, T. Monro, W. Berlardi, K. Furusawa, J. Lee, and D. Richardson, "2R-regenerative all-optical switch based on a highly nonlinear holey fiber," *Optics Letters*, vol. 26, pp. 1233-1235, 2001.

[11] M. Y. Chen, "Polarization and leakage properties of large-mode-area microstructured core optical fibers," *Optics Express*, vol. 15, no. 19, pp. 12498-12507, 2007.

[12] A. Ferrando, E. Silvestre, P. Andres, J. Miret, and M. Andres, "Nearly zero ultraflattened dispersion in photonic crystal fibers," *Optics Letters*, vol. 25, pp. 790-792, 2000.

[13] P. St. J. Russell, "History and future of photonic crystal fibers," *Optical Fiber Communication Conference*, USA, March 22-26, 2009.

[14] P. St. J. Russell, "Photonic crystal fibers: A historical account," *IEEE LEOS Newsletter*, vol. 21, pp. 11-15, Oct. 2007.

[15] B. Zsigri, J. Laegsgaard, and A. Bjarklev, "A novel photonic crystal fiber design for dispersion compensation," *Journal Optics A: Pure Applied Optic*, vol. 6, no. 7, pp. 717-720, Jul. 2004.

[16] J. C. Knight, T. A. Birks, P. St. J. Russel, and D. M. Atkin, "All-silica single-mode optical fiber with photonic crystal cladding," *Optics Letters*, vol. 21, no. 19, pp. 1547-1549, 1996.

[17] J. C. Knight, T. A. Birks, D. M. Atkin, and P. St. J. Russell, "Pure silica single mode fiber with hexagonal photonic crystal cladding," *Optical Fiber Communication Conference*, vol. 2, pp. 305-330, 1999.

[18] R. R. Musin, and A. M. Zheltikov, "Designing dispersion-compensating photonic-crystal fibers using a genetic algorithm," *Optical Communication*, vol. 281, no. 4, pp. 567-572, Feb. 2008.

[19] S. G. Li, X. D. Liu, and L. T. Hou, "Numerical study on dispersion compensating property in photonic crystal fibers," *Acta Physics Sin.*, vol. 53, no. 6, pp. 1880-1886, 2004.

[20] F. Gerome, J. L. Auguste, S. Fevrier, J. Maury, J. M. Blondy, and L. Gasca, "Dual concentric core dispersion compensating fiber optimized for WDM application," *Electronics Letters*, vol. 41, no. 3, pp. 116-117, Feb. 2005.

[21] M. Selim Habib, M. Samiul Habib, S. M. A. Razzak, Y. Namihira, M. A. Hossain, and M. A. G Khan, "Broadband dispersion compensation of conventional single mode fibers using microstructure optical fibers," Optik-International Journal for Light and Electron Optics, vol. 124, no. 19, pp. 3851–3855, Oct. 2013.

[22] S. K. Varshney, N. J. Florous, K. Saitoh, and M. Koshiba, "Numerical investigation and optimization of a photonic crystal fiber for simultaneous dispersion compensation over S+C+L wavelength bands," *Optical Communication* , vol. 274, no. 1, pp. 74-79, Jun. 2007.

[23] F. Begum, Y. Namihira, S. M. A. Razzak, S. F. Kaijage, N. H. Hai, T. Kinjo, K. Miayagi, and N. Zou, "Novel broadband dispersion compensating photonic crystal fibers: Applications in high speed transmission," *Optics & Laser Technology*, vol. 41, no. 6, pp. 679-686, Sep. 2009.

[24] S. F. Kaijage, Y. Namihira, N. H. Hai, F. Begum, S. M. A. Razzak, T. Kinjo, K. Miayagi, and N. Zou, "Broadband dispersion compensating octagonal photonic crystal fiber for optical communication applications," *Japanese Journal of Applied Physics*, vol. 48, 2009.

[25] M. Chen, Q. Yang, T. Li, M. Chen, and N. He, "New high negative dispersion photonic crystal fiber," *International Journal for Light and Electron Optics*, vol. 121, no. 10, pp. 867-871, Jun. 2010.

[26] F. Gerome, J. L. Auguste, and J. M. Blondy, "Design of dispersion compensating fibers based on a dual concentric core photonic crystal fiber," *Optics Letters*, vol. 29, no. 23, pp. 2725-2727, Dec. 2004.

[27] N. Ehteshami, and V. Sathi, "A novel broadband dispersion compensating square-lattice photonic crystal fiber," *Optical and Quantum Electronics*, vol. 44, no. 6, pp. 323-335, Jul. 2012.

CHAPTER II

Fundamentals of Photonic Crystal Fiber

2.1 Introduction

Photonic crystal fiber (PCF), also known as microstructured optical fiber (MOF) or holey fiber (HF) is a new class of optical fiber based on the properties of photonic crystals made of periodic optical nanostructures that affect the motion of photons. Photonic crystal fibers have recently made great interest in the scientific community because of providing the innovative ways to control and guide light which is not obtainable with conventional optical fibers. It has also the ability to confine light even in hollow cores. Due to its numerous properties, PCF has driven an exciting and irrepressible research activity all over the World in both telecom and non-telecom sector. For example, PCF is finding application in telecom sector including fiber-optic communications, fiber lasers, nonlinear devices, high-power transmission and then touching non-telecom sector such as biology, sensing, metrology, spectroscopy, microscopy, astronomy and micromachining. The term "photonic-crystal fiber" was coined by Philip Russell, pioneer of this research field after the invention of first silica-air microstructure of hexagonal structure in 1995-1996.

2.2 Construction of PCF

PCF is a microstructured single material optical fiber in which microscopic array of air channel run down the entire length of fiber [1]. These air-holes in the silica background constitute the cladding and thus make low refractive index profile in cladding. The background material in PCF is usually undoped silica. On the other hand, the core is normally formed either by removing a central air-hole from the whole structure or by creating a larger air-hole in its position. PCF structure with missing air hole in the core leads to solid core which forms high index profile in the core than cladding. This type of fiber structure is called high index core (HIC) or index-guiding (IG) PCF. Fiber structure with a placement of air hole in the core is called a hollow core (HC) or low index core (LIC) or photonic band gap (PBG) PCF. However, the solid core PCF first demonstrated by Philip Russell consisted of a hexagonal lattice of air holes in a silica in 1996 whereas hollow core PCF with a hexagonal lattice of air holes was first discovered by the same scientist Philip Russell in 1999 [1]. Fig. 2.1 shows cross sectional views of both the high

index and low index core PCFs. In the figure, air holes are represented by small unfilled circles. The absence of an air hole is denoted by a dotted small circle. Inclusions of air-holes in the PCF offer a variable index-contrast between the core and the cladding which is achieved by changing dimensions of holes and cladding geometry. Thus, PCFs have a number of design freedom namely air-hole diameter, air-hole to air hole distance (the pitch), core radius, and number of rings. Since the guiding properties of optical fibers depend on the refractive index and the refractive index of PCF depends on those design freedoms, application specific guiding properties can be achieved by modulating those parameters [2].

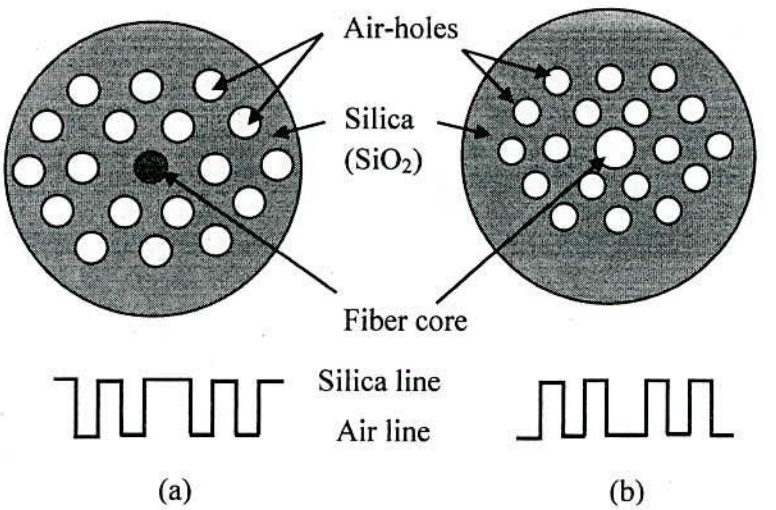

Fig. 2.1 Schematic cross sections and index-profiles of (a) IG-PCF (the dotted circle in the center indicates an omitted air-hole) and (b) HC or PBG PCF (the larger circle in the center represents the hollow core).

Index-guiding PCF with a solid glass region within a lattice of air-holes is shown in Fig. 2.1 which offers a lot of new opportunities not only for applications related to fundamental fiber optics. These opportunities are related to some special properties of the photonic crystal cladding which are due to the large refractive index contrast and the two-dimensional nature of the microstructure. As a result, guiding properties can be significantly altered and thus controlled the dispersion, dispersion slope, effective dispersion, birefringence, confinement loss, effective area and so on. Photonic bandgap PCF is shown in Fig. 2.1 (b) where the PCF core region has a lower refractive index than

the surrounding photonic crystal cladding. PCF with a low index core are created by introducing a defect in the photonic crystal structure, for example, an extra air-hole.

2.3 Classification of different PCF

Depending on the light guiding mechanism, PCFs is generally classified into two main categories, i.e., index guiding PCF (IG-PCF) and hollow core (HC) or photonic bandgap (PBG) PCF. However these two types of PCF can further be classified into a number of other types based on the dimensions of the fiber parameters, structures, and specific guiding properties. Upon them, IG-PCF can be broadly classified as

2.3.1 Highly nonlinear (HNL) fiber:

Core dimensions of this type of PCF are made very small so as to provide tight mode field confinement.

2.3.2 Large mode area (LMA) fiber:

Core dimensions of this type of PCF are made larger which exhibits small refractive index contrast and allow spreading out of the guiding light to provide a larger effective area.

2.3.3 Hole assisted PCF (HA-PCF):

This type of IG-PCF consists of doped core i.e. high index material doped silica surrounded by holey cladding.

2.3.4 High numerical aperture (HNA) fiber:

It consists of microstructure cladding surrounded by a ring of air-holes with larger dimensions.

On the other hand, PBG-PCF is classified as air-guiding (AG), HC fibers, low index core (LIC) fibers, or Bragg fibers. PCF can again be of another type namely polarization maintaining (PM) fibers having either a stress applying part or an asymmetric cladding structure to maintain a linear state of polarization. Again, likewise a conventional fiber, PCF is also classified as single mode or multi-mode fibers depending on the number of modes supported by a particular PCF either IG or PBG. All these types of microstructure PCF are shown in Fig. 2.2.

2.4 Light guiding mechanism of PCF

In order to form a guided mode in an optical fiber, it is necessary to introduce light into the core. PCF generally guides light using two mechanisms namely total internal reflection

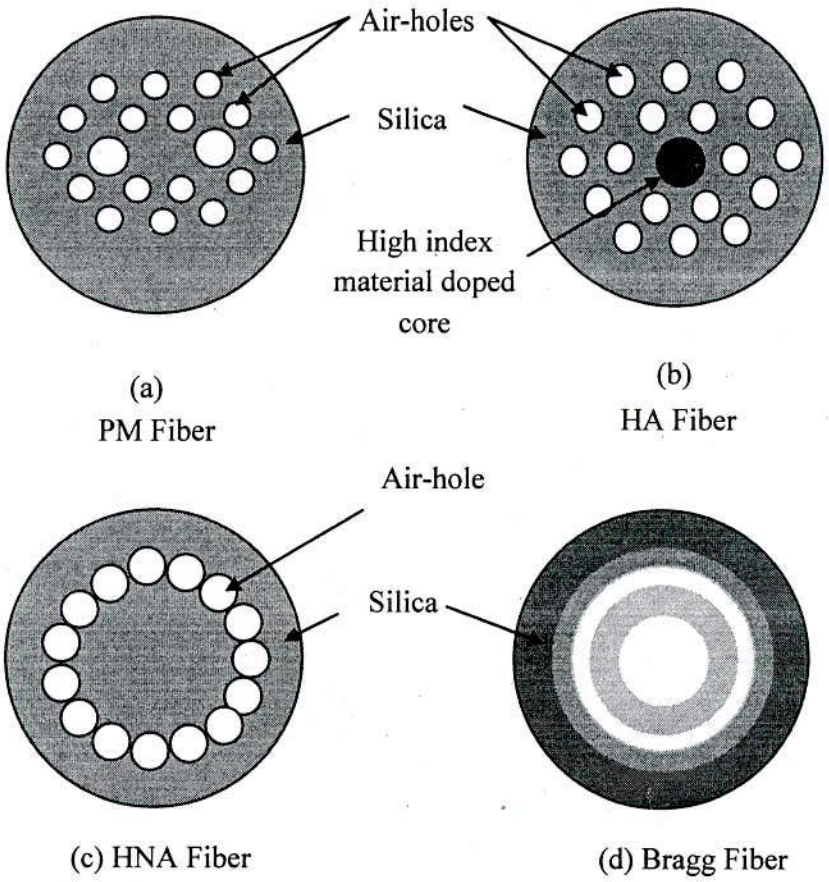

Fig. 2.2 Types of PCFs (a) PM-PCF, (b) HA-PCF, (c) HNA-PCF, and (d) Bragg Fiber

(TIR) and PBG mechanism. However, IG-PCF guides light through a form of total internal reflection (TIR) called modified TIR where a two-dimensional photonic crystal works as a fiber cladding and refractive index of core remains higher than refractive index of cladding. The guiding mechanism is defined as "modified" because the cladding refractive index is not a constant value than that of the standard optical fibers rather it changes significantly with the wavelength. In the contrary, PBG-PCF guides light via the mechanism of diffraction rather than total internal reflection [3]. Thus, light of any wavelength within that range cannot escape from the core and in analogy with electronic band-gap materials, cladding structure is called a photonic crystal and the wavelength range over which light is confined within the hollow core is called the band-gap of the material. Fig. 2.2(a) shows that IG-PCF generally omits a single air-hole from the structure. This type of PCFs can also have a high index material (e.g. Ge) doped core. In either case, the core must have a high refractive index ($n_{co} > n_{cl}$) than that of effective refractive index of the cladding. Unlike IG-PCFs, PBG PCFs have a hollow core ($n_{co} < n_{cl}$)

which is generally created by placing a larger air-hole in the center as shown in Fig.2.2 (d).

2.5 Difference between PCF and conventional fiber

An ordinary optical fiber is made of a core which has a higher refractive index than that of the cladding as shown in Fig. 2.3 (b). The refractive index of the core is made higher than that of the silica cladding by doping a high refractive index material in the core region. Thus Germanium is generally used for increasing the refractive index whereas Fluorine is commonly used material for decreasing the refractive index. In contrast, PCF is a single material fiber that contains tiny air holes in a silica background as shown in Fig 2.3 (a). Index contrast between the core and the cladding of conventional fibers is very low but PCF offers a wide possibility to control the index contrast between the core and the photonic crystal cladding by simply modulating the cladding parameters. This is the primary difference between the two fibers for which novel and unique optical properties can be achieved significantly using PCF [4].

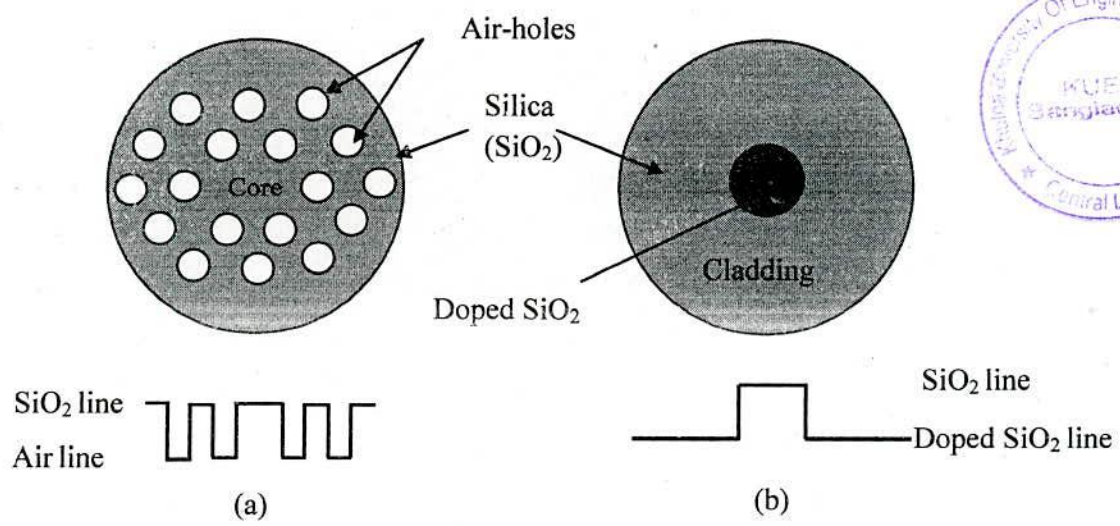

Fig. 2.3 Schematic cross sections and index-profiles of (a) PCFs (a missing air-hole in the center represents the core) and (b) Ordinary fibers.

2.6 Guiding properties of the PCF

In the following subsections, wavelength dependent response of chromatic dispersion, birefringence, confinement loss, mode field diameter, effective area and single/multi-mode response of PCF are discussed.

2.6.1 Chromatic dispersion

An important transmission characteristic of an optical fiber is dispersion, which describes wavelength-dependent transmission delays [5]. However, an optical pulse broadens during transmission through the fiber in the presence of dispersion which ultimately limits transmission speed as well as distance. Transmission media having such a property are termed dispersive media. In addition, an optical pulse passing through the dispersive media causes separation of the transmitted pulse into its spectral components which will overlap with each other at the output end of the optical fiber. Thus overlapped optical pulses at the output of the transmission fiber may not be recovered and hence the transmitted information will be lost. Moreover, dispersion is sometimes called chromatic dispersion to emphasize its wavelength-dependent nature [6]. Dispersion in an optical fiber has two components such as material dispersion and waveguide dispersion. Material dispersion comes from the wavelength-dependent refractive index of the material used to make optical fibers and it slightly varies from fiber to fiber. Waveguide dispersion on another hand comes from wavelength-dependent guiding properties of the optical waveguide i.e. the speed of a wave in a waveguide depends on its frequency and can be varied significantly by a waveguide design. However, a similar phenomenon is modal dispersion, caused by a waveguide having multiple modes at a given frequency, each with a different speed. A special case of this is polarization mode dispersion (PMD) which comes from a superposition of two modes that travel at different speeds due to random imperfections that break the symmetry of the waveguide.

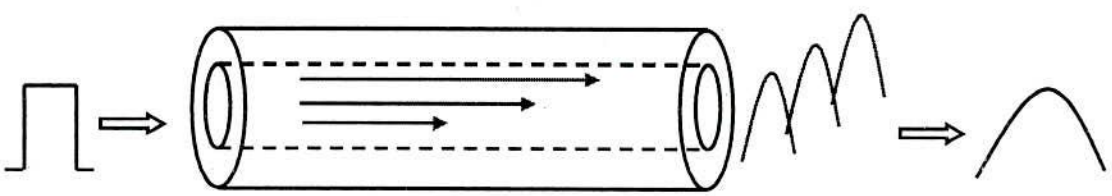

Fig. 2.4 Dispersion phenomena in an optical fiber.

2.6.2 Birefringence

Birefringence is the optical property of a material having a refractive index that depends on the polarization and propagation direction of light. These optically anisotropic materials are said to be birefringent. When a ray of light is incident upon a birefringent fiber, it is split by polarization into two orthogonal polarization modes (x-polarization mode and y-polarization mode) which will travel at a different speed due to the slight difference in refractive index between the two orthogonal modes. Hence, birefringence is often quantified as the maximum difference of refractive indices between two orthogonal polarization modes exhibited by the fiber. Birefringent photonic crystal fiber (PCF) can be achieved by having asymmetric core. This increases the effective index difference between the two orthogonal polarization modes. When, in a fiber, symmetry breaking part is added intentionally so that the birefringence is no longer governed by the random core size and shape, it is called a polarization maintain (PM) fiber. In such a case, intentionally introduced birefringence weakens the random polarization effect thus maintain a single polarization. The typical value of birefringence is of the order 10^{-4} for conventional PM fibers. PM fibers can have polarization beat lengths of a few centimeters or even only a few millimeters. A fiber having short beat length exhibits strong birefringence and even sub-millimeter beat lengths are possible with some PCFs showing strong birefringence than that of conventional PM fibers [7]. PM fibers are used in special applications including sensing application.

2.6.3 Confinement loss

Confinement loss may be defined as the leakage due to the similar refractive index between core and cladding. It is a phenomenon whereby part of the guided light penetrated to the cladding region causing signal degradation. Similar to the conventional fibers, PCF guides light based on the TIR mechanism. However PCF supports three kinds of modes such as the guided mode, radiation mode and leaky mode [8]. Among these modes confinement loss is treated as the loss of leaky modes. In PCF, the core and the cladding effective indexes are the same except that there are a finite number of air-holes in the cladding. If the confinement loss is higher, then signal will be degraded through the fiber. Actually air-holes in the cladding region limit the optical field penetration in the cladding region. There will be no confinement loss in PCFs if there is infinite number of air-holes in the cladding region [9]. This loss depends on the size of the core, air-hole dimension,

pitch, and number of rings in the cladding. Fig. 2.5 illustrates confinement losses in PCFs. It shows that the guiding light is penetrating to the cladding region through air-holes.

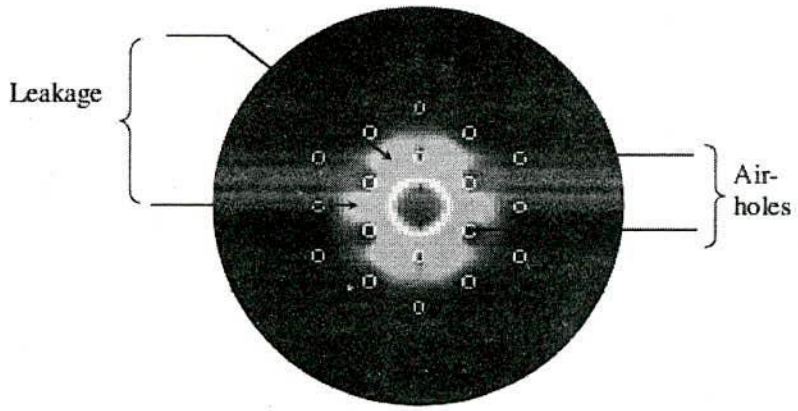

Fig. 2.5 Confinement losses in index-guiding PCF.

2.6.4 Mode field diameter and effective area

In fiber optics, the mode field diameter (MFD) is an expression of distribution of the irradiance that is the optical power per unit area across the end face of a single-mode fiber. The most popular model used in single mode fibers for the beam intensity is a Gaussian distribution [1, 10-11]. For a Gaussian intensity distribution in a single-mode optical fiber, effective area is the area where the beam intensity drops to 13.5% of the maximum value and the diameter of which is called the mode field diameter (MFD) and can be calculated directly from the electric field distribution by using the Petermann-II definition [12].

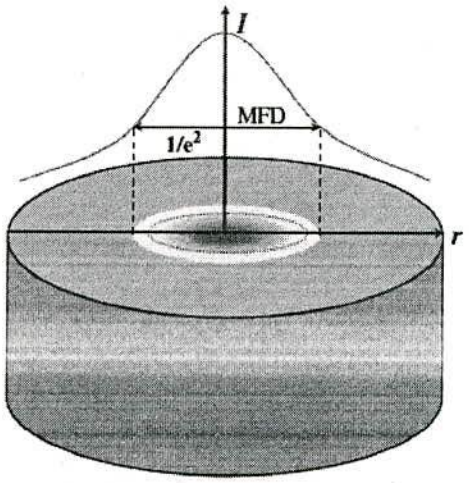

Fig. 2.6 Gaussian intensity distribution in a single-mode optical fiber.

2.6.5 Single mode or multimode response

Conventional fibers can operate single-mode or multi-mode depending mostly on the dimension of the core. PCFs, on the other hand, can be designed for endlessly single-mode operation by proper choice of air-hole dimension and pitches. For a uniform cladding, PCFs show endlessly single mode response as long as the d/Λ ratio remains within a 0.45, above the value may result in either single-mode or multimode operation. Using the V parameter of PCFs, it is possible to determine the single mode response.

2.7 Applications of PCF

Since, PCF provides new or improved features, beyond what conventional optical fiber offers, they are finding an increasing number of applications in both the linear and the nonlinear regimes. Solid core PCF or IG-PCF can be used to meet certain requirement of the present day optical communication system such as high birefringence, ultrahigh nonlinearities, tailoring dispersion, and LMA fibers. For example, birefringent fibers are used to maintain the polarization states in optical devices and subsystems. Thus by slightly changing the air-hole geometry, it is possible to produce levels of birefringence that exceed the performance of conventional birefringent fiber by an order of magnitude. Therefore, highly birefringent PCFs are being used in different types of sensors including remote environmental sensors and bio-sensors [13]. On the other hand, dispersion which is a crucial factor of telecommunication system can be changed and controlled largely with the PCF than conventional fiber. Thus, PCF with large negative dispersion are suitable for dispersion compensation while LMA-PCFs are suitable for telecommunications and high power application [14]. HNL-PCF and near zero dispersion flat PCF are being used in optical parametric amplification, all optical signal processing, soliton pulsed systems, and supercontinuum generation [15]. Furthermore, PCFs are becoming suitable for many other applications in present day optical systems and they are equally potential for future all optical systems.

2.8 Conclusion

To investigate the properties of PCF as broadband dispersion compensator, some preliminary concepts of PCF has been discussed in brief including PCF construction, refractive index profile, light guiding mechanism of PCF, types of PCF and difference between conventional optical fiber and PCF. In addition, some guiding properties of PCF

have been discussed in details including chromatic dispersion, effective mode area, confinement loss, birefringence, and single and multi-mode response. Finally, application of PCF has been presented.

References

[1] P. St. J. Russell, "Photonic Crystal Fibers," Science, vol. 299, no. 5605, pp. 358-362, Jan. 2003.

[2] J. A. Buck, Fundamentals of Optical Fibers, John Wiley & Sons Inc., USA, 2nd Edition, 2004P. St. J. Russell, "Photonic crystal fibers," *Science,* vol. 299, pp.358-362, 2003.

[3] J. C. Knight, J. Broeng, T. A. Birks and P. St. J. Russell, "Photonic band gap guidance in optical fibers," *Science,* vol. 282, pp.1476-1478, 1998.

[4] S. V. Kartalopoulos, DWDM Networks, Devices, and Technology, John Wiley & Sons Inc., USA, 2003.

[5] B. Max and W. Emil, Principles of Optics. Cambridge, Cambridge University Press, pp. 14–24, Oct. 1999.

[6] R. A. Correa and J. C. Knight, "Specialty Fibers: Novel process eases production of hollow core fiber," Laser Focus World, Vol. 44, No. 05, May 2008.

[7] J. C. Knight, T. A. Birks, P. St. J. Russel, and D. M. Atkin, "All-silica single-mode optical fiber with photonic crystal cladding," Optics Letters, vol. 21, no. 19, pp. 1547-1549, 1996.

[8] M. Y. Chen, "Polarization and leakage properties of large-mode-area microstructured-core optical fibers," Optics Express, vol. 15, no. 19, pp. 12498-12507, 2007.

[9] K. Saitoh, A. Ferrando, E. Silvestre, P. Andres, J. Miret, and M. Andres, "Nearly zero ultraflattened dispersion in photonic crystal fibers," Optics Letters, vol. 25, pp. 790-792, 2000.

[10] J. C. Knight, "Photonic crystal fibers," Nature, vol. 424, pp. 847-851, Aug. 2003.

[11] L. P. Shen, W. P. Hung, and S. S. Jian, "Design and optimization of photonic crystal fibers for broadband dispersion compensation," IEEE Photonics Technology Letters, vol. 15, no. 4, pp. 540-542, Apr. 2003.

[12] T. A. Birks, J. C. Knight, and P. St. J. Russell, "Endlessly single-mode photonic crystal fiber," Optics Letters, vol. 22, no. 13, pp. 961-963, July 1997.

[13] G. P. Agrawal, Fiber-Optic Communication Systems, John Wiley & Sons Inc., USA, 2nd Edition, 1997.

[14] G. P. Agrawal, Fiber-Optic Communication Systems, John Wiley & Sons Inc., USA, 3rd Edition, 2002

[15] G. P. Agrawal, Nonlinear Fiber Optics, Academic Press, USA, 2nd Edition, 1995.

CHAPTER III

Numerical Modeling and Analysis of DC-PCFs

3.1 Introduction

This chapter presents different modeling methods and necessary equations for the numerical computation of PCF's modal properties. Numerical modeling plays a vital role for theoretical studies of PCF because of the complex nature of the electromagnetic waves. However, various wave guiding structures that utilize the arrangement of microstructured holes [1] or thin layers [2] have been realized due to the introduction of PCF. The varieties of hole shapes and their arrangements in PCF demand the use of numerical methods that can handle arbitrary cross-sectional shapes to analyze guiding properties of the PCF precisely. Besides, the existence of interfaces with high refractive index-contrast between the solid host material and air holes calls for the use of the vectorial wave equations to accurately model the PCF structure.

3.2 Existing numerical methods

Optical signal is a form of electromagnetic wave which has electric and magnetic fields that are orthogonal to each other. However, the wave equations in fiber-optics are based on Maxwell's equations. Various computational methods individually or in combination used to solve wave equations. Several methods such as plane wave expansion method (PWEM) [3] suitable for periodic structures, localized function method (LFM) [4], beam propagation method (BPM) [5], boundary element method (BEM) [6], and finite-difference method (FDM) [7] in time domain [8] or frequency domain [9] has been proposed to date for numerical design tools. Specifically, a highly accurate semi-analytical multi-pole method (MPM) suitable for predicting leakage losses of PCFs [10] has been developed to model PCF with circular air holes. PWEM assumes an infinite periodic index profile and treats the unit cell or super cell by applying the Bloch boundary conditions. Such PWEM is adequate for index-guiding PCF with many periodic air holes in the cladding. However, the artificial periodic boundary condition and super cell approach are not very suitable for many real fiber structures with a finite number of air holes. On the other hand, the LFM based on Galerkin method has been widely used for waveguide analysis including both scalar and vectorial problems. However, this method generally

involves integrations which are computational intensive and the convergence is generally a problem. In contrast, the scalar wave analysis methods are not accurate to predict their guiding properties of PCF because of high refractive index contrast between the undoped silica and air. As a result, a full-vector approach is required to analyze the wave propagation properties through the PCF. Among the full vector methods, finite element method (FEM) is a powerful numerical tool for waveguide problems which can handle the vectorial wave-equation transparently and hence it is suitable for a wave guiding structure with high index-contrast. Hence, the FEM is very suitable for handling structures with a complicated geometry. Earlier, FEM has been used to successfully investigate of PCF dispersion [11], parametric amplification [12] and nonlinear properties [13]. In addition, the complex FEM formulation has been very useful to evaluate the PCF leakage or confinement losses due to the finite number of air-hole rings in the cladding lattice [14]. As a result, FEM is expected to be more accurate and appropriate candidate to analyze the various properties of PCF structure compared to other existing numerical methods. In this thesis, the COMSOL Multiphysics 4.2 software based on the FEM is used for PCF's modal computations.

3.3 Formulation of FEM method

Dispersion properties of the PCF presented in this thesis have been determined using the COMSOL Multiphysics 4.2 software based on FEM. Using FEM, the PCF cross section, with the finite number of air holes, is divided into homogeneous subspaces. However, these subspaces are triangles that allow a good approximation of the circular structures of PCF. Afterward, each adjacent sub-space is solved using Maxwell's equations. On the other hand, the leakage loss of a mode can be represented by the imaginary part of its complex propagation constant. To model the leakage, an open boundary condition has to be used which produces no reflection at the boundary. The perfectly matched layer (PML) are so far the most efficient absorption boundary condition for this purpose by which propagation characteristics of leaky modes in PCF as well as even both dispersion and loss properties can be accurately evaluated [15, 16]. However, the waveguide is encompassed by PML layers followed by a layer of perfect electric conductor (PEC) or zero boundaries. The modes leaking out of the fiber will be absorbed efficiently by the PML with very small reflections. Using the anisotropic PML, from Maxwell's curl equations, the full vectorial equation can be written as [15]

$$\nabla \times \left([s^{-1}] \nabla \times \vec{E} \right) - k_0^2 n_{eff}^2 [s] \vec{E} = 0 \qquad (3.1)$$

$\vec{E}$ denotes the electric field and $k_0 = \frac{2\pi}{\lambda}$ is the wave number in the vacuum, λ being the wavelength, n_{eff} is the effective refractive index, [s] is the PML matrix and [s^{-1}] is an inverse matrix of [s]. Finally, the effective refractive index of PCF is solved from the above Maxwell's curl equation.

3.4 Determination of the modal properties of PCF

The designed PCF is simulated to find the effective refractive index, n_{eff} using COMSOL Multiphysics 4.2 based on FEM. Once the effective refractive index, n_{eff} is obtained, the modal properties of the PCF such as chromatic dispersion, dispersion slope and relative dispersion slope (RDS), effective dispersion, confinement loss, birefringence, effective area and effective V-parameter can be easily calculated using the following equations.

3.4.1 Chromatic dispersion

The chromatic dispersion $D(\lambda)$ of the PCF is calculated from the following differential equation formulated in [17].

$$D(\lambda) = -\frac{\lambda}{c} \frac{d^2 \, \mathrm{Re}[n_{eff}]}{d\lambda^2} \quad \text{ps/(nm.km)} \qquad (3.2)$$

In above equation, $\mathrm{Re}[n_{eff}]$ is the real part of effective refractive index n_{eff}, λ is the wavelength, c is the velocity of light in vacuum. The total dispersion $D(\lambda)$ is algebraic summation of material dispersion and waveguide dispersion. Thus, the material dispersion is calculated from the three term Sellmeier equation and is directly included in the FEM calculation process. However, it is mostly determined by the wavelength dependence property of the fiber material. Moreover, the waveguide dispersion strongly depends on the silica-air structure itself [18] and can be altered significantly by modulating some parameters like geometry of the air holes, pitch, and air-hole diameters. Hence, the chromatic dispersion $D(\lambda)$ of PCFs is related to those additional design parameters and by optimizing these parameters, suitable guiding properties can be achieved for dispersion compensation of SMF.

3.4.2 Dispersion slope and RDS

The dispersion slope (DS) of the PCF can be determined by differentiating the dispersion, $D(\lambda)$ with respect to wavelength, λ whereas the RDS is found by taking the ratio of DS to dispersion. The equations of DS and RDS is given as follows [19]

$$DS(\lambda) = \frac{dD(\lambda)}{d\lambda} \quad \text{ps/(nm}^2\text{.km)} \tag{3.3}$$

$$RDS = \frac{DS(\lambda)}{D(\lambda)} \quad \text{nm}^{-1} \tag{3.4}$$

$$RDS_m = RDS_n = \frac{DS_m(\lambda)}{D_m(\lambda)} = \frac{DS_n(\lambda)}{D_n(\lambda)}) \tag{3.5}$$

The RDS is used to judge dispersion compensating capability of a DCF over a range of wavelengths. Hence, to compensate the accumulated dispersion of the SMFs over a range of wavelength, the condition of Eq. (3.5) must be satisfied where RDS_m and RDS_n represents the RDS of SMF and DCF respectively. Once the RDS of the DCF is close to that of the SMF, the design of the broadband DCF will be accomplished. However, the RDS of SMF is 0.0036 nm^{-1} at 1550 nm.

3.4.3 Effective dispersion

If a fiber link consists of transmission fiber mainly SMF of length L_m with the dispersion of $D_m(\lambda)$ and a DCF of length, L_n with the dispersion of $D_n(\lambda)$, then the effective dispersion, $D_e(\lambda)$ on the fiber link after compensating the SMF of length, L_m can be calculated using the following equation [19].

$$D_e = \frac{D_m(\lambda)L_m + D_n(\lambda)L_n}{L_m + L_n} \quad \text{ps/(nm.km)} \tag{3.6}$$

It should be mentioned here that the effective dispersion of DCF should be lower that ± 0.8 ps/(nm.km) to deploy in high bit rate transmission system [17, 19].

3.4.4 Confinement loss

Confinement loss indicates light confinement ability of the optical fiber within its core region. In PCF, confinement of light within the core region increases appreciably with the increase of number of air-hole rings and subsequently the confinement loss is reduced. On the other hand, there is a design freedom in PCF to choose the suitable number of air-hole

rings to keep the confinement loss within the desired value. However, the confinement loss in dB/m can be defined as [19]

$$L_c = 8.686 \times \frac{2\pi}{\lambda} \times \mathrm{Im}[n_{eff}] \tag{3.7}$$

where $\mathrm{Im}[n_{eff}]$ represents the imaginary part of the wavelength dependent refractive index and λ is the wavelength in the free space. The complex refractive index of fundamental mode can also be found by FEM.

3.4.5 Birefringence

In PCF, the birefringence properties are imperative for polarization maintaining applications. PCF with polarization maintaining (PM) properties are essential in applications such as in eliminating the effect of polarization mode dispersion (PMD) and in stabilizing the operation of optical devices, and can also be used in sensing applications. The birefringence is defined as [19]

$$B = \left| n_x - n_y \right| \tag{3.8}$$

Where, n_x and n_y are the mode indices of the two orthogonal polarization fundamental modes. It should be pointed out that, the conventional PM fiber exhibits a modal birefringence of about 5×10^{-4} and is insufficient to eliminate the effect of PMD. Hence, birefringence of the DCF should be higher to eliminate the PMD of SMF. However, the birefringence of the PCF can be increased significantly by breaking the symmetry of the PCF core [19].

3.4.6 Effective area

The effective area A_{eff} in μm^2 of the proposed PCF is obtained from [17] and is given by

$$A_{eff} = \frac{\left(\iint |E|^2 \, dxdy \right)^2}{\iint |E|^4 \, dxdy} \tag{3.9}$$

where E is the electric field vectors in the medium.

3.4.7 Single and multimode response

Properties of standard fibers are often parameterized by the so-called V-parameter. Such V-parameter helps to determine whether a fiber is single or multimode fiber. However, the tradition of determining single and multimode response from V parameter stems from

analysis of the step-index fiber (SIF). In contrast, due to the constructional difference between SIF and PCF, the equation to find the V parameter should be different from that of SIF and the equation of effective V parameter is given by [20]

$$V_{eff} = k\Lambda F^{\frac{1}{2}}(n_{eff}^2 - n_a^2)^{\frac{1}{2}} \tag{3.10}$$

where $k_0 = \frac{2\pi}{\lambda}$ is the wave number in the vacuum, F is the air-filling fraction, Λ is the pitch, n_{eff} is the effective index, and n_a is the refractive index of the air. However, the single-mode regime is characterized by $V_{eff} < \pi$ [21]. Once the normalized effective V parameter is obtained as $V_{eff} < \pi$ for certain wavelength bands, then the fiber will act as a single mode fiber (SMF) over that wavelength bands.

3.5 Conclusion

As a part of numerical modeling of PCF, several existing modeling methods of PCF have been discussed in brief. Presently, FEM has been extensively used to model the PCF which has been discussed in this thesis. In this thesis COMSOL Multiphysics 4.2 software based on FEM has been used to model PCF. Finally, some equations for numerical computations have been presented to investigate the properties of PCF as broadband dispersion compensator.

References

[1] P. St. J. Russell, "Photonic Crystal Fibers," *Science*, vol. 299, no. 5605, pp. 358-362, Jan. 2003.

[2] Y. Fink, "Guiding optical light in air using an all-dielectric structure," *Journal of Lightwave Technology*, vol. 17, pp. 2039-2041, 1999.

[3] A. Ferrando, E. Silvester, J. J. Miret, P. Andrés, and M. V. Andrés, "Full vector analysis of a realistic photonic crystal fiber," *Optics Letters*, vol. 24, no. 5, pp. 276–278, Mar. 1999.

[4] T. M. Monro, D. J. Richardson, N. G. R. Broderick, and P. J. Bennett, "Modeling large air fraction holey optical fibers," *Journal of Lightwave Technology*, vol. 18, no. 1, pp. 50–56, Jan. 2000.

[5] F. Fogli, L. Saccomandi, and P. Bassi., "Full vectorial BPM modeling of index guiding photonic crystal fibers and couplers," *Optics. Express*, vol. 10, no. 1, pp. 54–59, Jan. 2002.

[6] T. L. Wu and C. H. Chao, "Photonic crystal fiber analysis through the vector boundary-element method: Effect of elliptical air hole," *IEEE Photonics Technology Letters*, vol. 16, no. 1, pp. 126–128, Jan. 2004.

[7] Z. Zhu and T. G. Brown, "Full-vectorial finite-difference analysis of microstructured optical fibers," *Optics Express*, vol. 10, no. 17, pp. 853–864. Aug. 2002.

[8] J. T. Lizier and G .E. Town, "Splice losses in holey optical fibers," *IEEE Photonics Technology Letters*, vol. 13, no. 8, pp. 794–796, Aug. 2001.

[9] P. Lusse, P. Stuwe, J. Schule, H.G. Unger, "Analysis of vectorial mode fields in optical waveguides by a new finite difference method," *Journal of Lightwave Technology*, vol. 12, pp. 487-494, 1994.

[10] T .P. White, B. T. Kuhlmey, R. C. Mc Phedran, D. Maystre, G. Renversez, C. M. de Sterke, and L. C. Botten, "Multipole method for microstructured optical fibers. I. Formulation," *Journal of Optical Society of America* , vol. 19, no. 10, pp. 2322–2330, Oct. 2002.

[11] F. Poli, A. Cucinotta, S. Selleri, and A. H. Bouk, "Tailoring of flattened dispersion in highly nonlinear photonic crystal fibers," *IEEE Photonics Technology Letters*, vol. 16, pp. 1065–1067, Apr. 2004.

[12] A. Cucinotta, F. Poli, and S. Selleri, "Design of erbium-doped triangular photonic crystal fiber based amplifiers," *IEEE Photonics Technology Letters*, vol. 16, pp. 2027–2029, Sept. 2004.

[13] M. Fuochi, F. Poli, S. Selleri, A. Cucinotta, and L. Vincetti, "Study of Raman amplification properties in triangular photonic crystal fibers," *IEEE Journal of Lightwave Technology*, vol. 21, pp. 2247–2254, July 2003.

[14] D. Ferrarini, L. Vincetti, M. Zoboli, A. Cucinotta, and S. Selleri, "Leakage properties of photonic crystal fibers," *Optics Express*, vol. 10, pp. 1314–1319, Nov. 2002.

[15] K. Saitoh and M. Koshiba, "Full-vectorial imaginary-distance beam propagation method based on a finite element scheme: Application to photonic crystal fibers," *IEEE J. Quantum Electron.*, vol. 38, no. 7, pp. 927–933, Jul. 2002.

CHAPTER IV

Design and Characterization of Broadband DC-PCF

4.1 Introduction

This chapter demonstrates the design methodology of broadband DCF using PCF and hence, describes the performance of the designed DCF as a dispersion compensator to compensate the accumulated dispersion of transmission fiber. This chapter also presents the condition of broadband dispersion and dispersion slope compensation. Firstly, C-PCF is designed to achieve the goal of broadband dispersion compensation of SMFs. However, simulation results reveal that although C-PCF gives high negative dispersion over a wide band but the birefringence is not enough high as to compensate the PMD. As a result, M-CPCF has been designed to achieve a large value of birefringence which leads to PMD compensation. Moreover, simulation results show that it is possible to use M-CPCF to compensate both chromatic dispersion and PMD. In addition, M-OPCF has been designed and simulated to observe the performance as dispersion compensator. Finally, a comparison has been made to show the performance of the designed DC-PCFs.

4.2 Requirements for broadband dispersion and dispersion slope compensation

Dispersion compensation is a technique to nullify the positive dispersion caused by the standard SMFs. It is usually done using DCF which shows negative dispersion characteristics than that of SMFs so as to achieve signal with zero dispersion at the output of transmission fiber. However, the use of negative-slope DCFs offer the simplest solution to dispersion compensation in high capacity WDM systems with a large number of channels. The equation of broadband dispersion compensation is given by [1]

$$D_m(\lambda_n)L_m + D_n(\lambda_n)L_n = D_t \tag{4.1}$$

where $D_m(\lambda_n)$ and $D_n(\lambda_n)$ are dispersion coefficient of SMF and DCF where λ_n is wavelength of n^{th} channel, L_m and L_n are the length of SMF and DCF respectively. For full compensation of the dispersion caused by SMF, the length of the DCF is selected such that total dispersion coefficient D_t=0 after dispersion compensation. Under this condition, the length of DCF will be as follows

$$L_n = -\frac{D_m L_m}{D_n} \tag{4.2}$$

The equation clearly shows that the length of DCF will be short only for high negative value of D_n. On the other hand, dispersion compensation over a wide range of wavelength requires dispersion and dispersion slope compensation at the same time for broadband communication system. Hence, the total dispersion slope DS_t is given as follows [2]

$$DS_t = DS_m L_m + DS_n L_n \tag{4.3}$$

where DS_m, DS_n are the dispersion slopes of the SMF and the DCF respectively. From Eq. (4.3), it is obvious that a negative dispersion slope of the DCF is necessary in order to achieve slope compensation. Thus, the condition for full slope compensation is that the relative dispersion slope (RDS), which is the ratio of dispersion slope to dispersion, of both fibers would have to be equal

$$RDS_m = RDS_n \tag{4.4}$$

where RDS_m and RDS_n are the relative dispersion slope of the standard SMF and the DCF. It should be pointed out that standard SMF exhibits RDS value of about 0.0036 nm^{-1} at λ=1.55 μm [2]. Once the RDS value of DCF is close to that of the SMF, the design of the broadband DCF is achieved.

4.3 Proposed DC-PCF models

In order to achieve the goals, we have modeled three DC-PCF structures for broadband dispersion compensation namely C-PCF [19], M-CPCF and M-OPCF [20]. C-PCF is designed with only circular air holes of different sizes for different air hole rings. However, it gives a good dispersion compensating properties but birefringence is not so high. To enhance the birefringence property of C-PCF, M-CPCF is offered which consists of both circular and elliptical air holes. Finally, M-OPCF is modeled with circular air holes in the cladding.

4.3.1 Structure of C-PCF

Fig. 4.1 represents air-hole distribution of the proposed dispersion compensating C-PCF. The proposed C-PCF contains five air-hole rings. Air hole 10 signifies 1st air hole of 1st air hole ring. Similarly, air hole 20, 30, 40 and 50 represent 1st air hole of 2nd, 3rd, 4th and 5th air hole ring respectively.

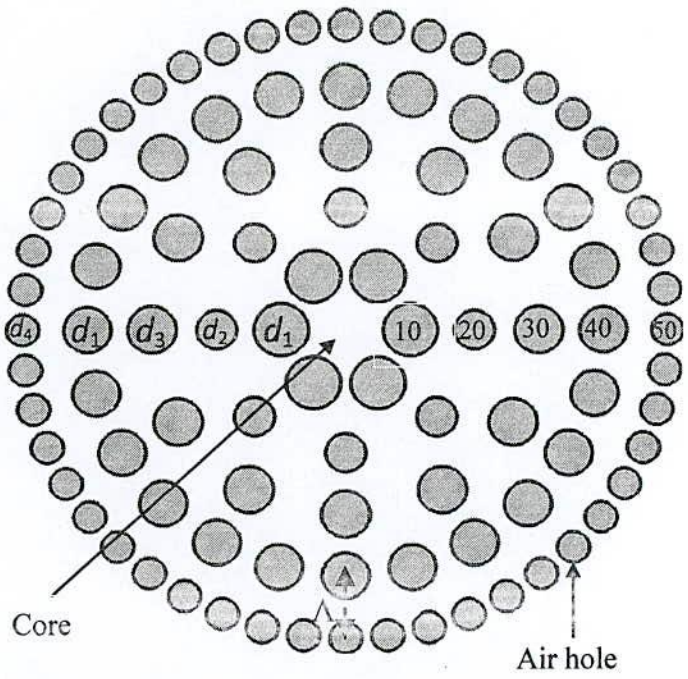

Fig. 4.1 Structure of the proposed C-PCF for broadband dispersion compensation.

The air-holes on the 1st ring are rotated at an angle of 60^0 from the center of the core while air-holes on the 2nd to 5th rings are rotated at an angle of 45^0, 30^0, 15^0, and 7.5^0 respectively. However, the number of air-holes of the proposed structure for rings 1, 2, 3, 4 and 5 are respectively 6, 8, 12, 24 and 48. The air hole diameter of 1st and 4th ring is d_1 while air-hole diameter of the 2nd, 3rd and 5th ring is selected as d_2, d_3 and d_4. The distance between the neighboring air holes of two adjacent air hole rings denoted as pitch and it is represented by Λ. For example, air hole 10 is neighbor of air hole 20 and thus the center to center distance between these two air holes is Λ whereas distance between other air holes is a function of Λ. However, the position of the air holes is designed with taking into account the center of the core of the proposed PCF as origin of cartesian coordinate system. Then, the position of air holes, (X_{Nn}, Y_{Nn}) in each ring will be determined as follows where N denotes the number of rings and n represents the total number of air holes in that ring. For instance, the position of air holes in 1st ring (N=1) can be designed using the following equation. In this case, the total number of air holes in the 1st ring, n would be 6 where n=0, 1, 2….5.

$$(X_{Nn}, Y_{Nn}) = (N \times \Lambda \times \cos(\frac{n\pi}{3}), N \times \Lambda \times \sin(\frac{n\pi}{3})) \quad (4.5)$$

Similarly, the position of all air holes in 2nd (N=2, n=8 where n=0, 1, 2....7), 3rd (N=3, n=12 where n=0, 1, 2....11), 4th (N=4, n=24 where n=0, 1, 2....23), and 5th (N=5, n=48 where n=0, 1, 2....47) rings can be determined using the following equations

$$(X_{Nn}, Y_{Nn}) = (N \times \Lambda \times \cos(\frac{n\pi}{4}), N \times \Lambda \times \sin(\frac{n\pi}{4})) \quad (4.6)$$

$$(X_{Nn}, Y_{Nn}) = (N \times \Lambda \times \cos(\frac{n\pi}{6}), N \times \Lambda \times \sin(\frac{n\pi}{6})) \quad (4.7)$$

$$(X_{Nn}, Y_{Nn}) = (N \times \Lambda \times \cos(\frac{n\pi}{12}), N \times \Lambda \times \sin(\frac{n\pi}{12})) \quad (4.8)$$

$$(X_{Nn}, Y_{Nn}) = (N \times \Lambda \times \cos(\frac{n\pi}{24}), N \times \Lambda \times \sin(\frac{n\pi}{24})) \quad (4.9)$$

However, the size (radius) of air holes of 1st to 5th rings can be determined using the normalized diameter, D_N, the ratio of air hole diameter, d_N to pitch, Λ.

$$\text{Radius of the air holes}, r = D_N \times \frac{\Lambda}{2} \quad (4.10)$$

where D_N is the normalized diameter of air holes of all rings where N=1, 2....5 and D_N varies from one air hole ring to another. On the other hand, the material of proposed C-PCF is taken to be silica except the air holes whose refractive index is 1. Thus, the effective refractive index, n_{eff} of the material is changed with operating wavelength. However, the wavelength dependent refractive index of the material is determined by Sellmeier equation [2].

4.3.2 Structure of M-CPCF

Fig. 4.2 represents the air hole arrangement of M-CPCF with optimized air-hole diameters d_1, d_2, d_3, pitch , Λ and ellipticity, η. However, the construction of the M-CPCF for broadband dispersion compensation is mostly identical with C-PCF except these elliptical air holes which have been used to enhance the dispersion compensating capability. Moreover, the proposed structure has two circular air-holes missing in the first ring and replaced by two elliptical air holes. It is expected that the birefringence of the proposed M-CPCF would be increased appreciably.

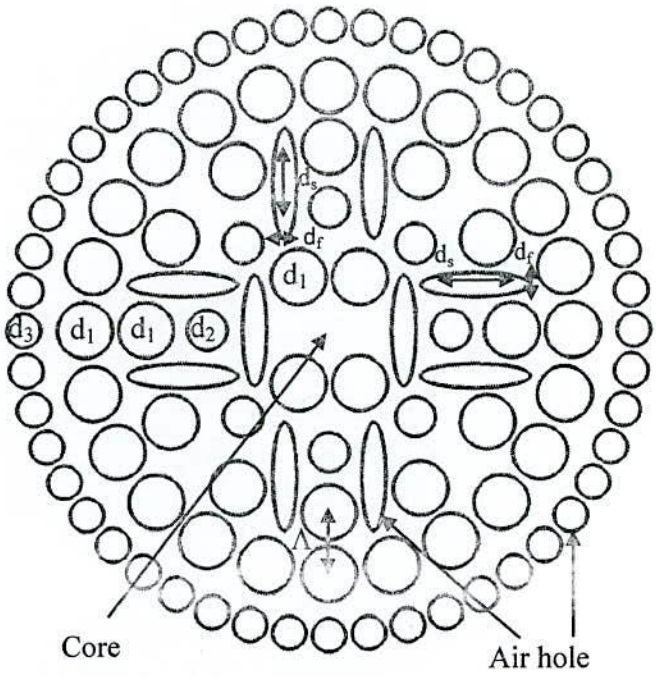

Fig. 4.2 Structure of the proposed M-CPCF for broadband dispersion compensation.

4.3.3 Structure of M-OPCF

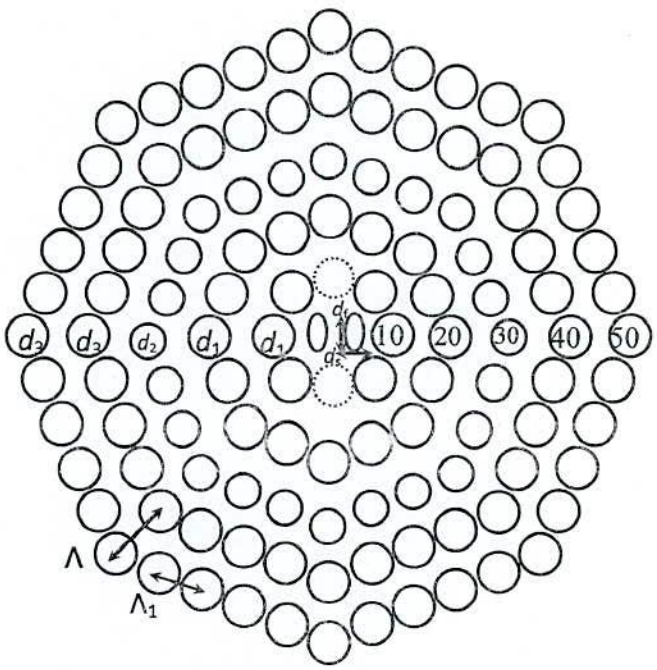

Fig. 4.3 Structure of the proposed M-OPCF for broadband dispersion compensation.

Fig. 4.3 shows the model of the proposed M-OPCF with optimized air-hole diameters d_1, d_2, d_3, pitch Λ, and ellipticity η. In contrast to conventional M-OPCF, the proposed structure has two air-holes missing in the first ring (the dotted circle). Pitch Λ is related to Λ_1 by the relation $\Lambda_1 \approx 0.765\Lambda$. The designed octagonal PCF has isosceles triangular unit lattices and hence more air-holes in the cladding region with the same numbers of rings than hexagonal PCF. This results in a higher air-filling ratio and a lower refractive index around the core, thereby providing strong confinement ability. We have also added two extra elliptical air-holes adjacent to the core to achieve high birefringence property. It is known that the size of the air-holes near the PCF core affects the dispersion characteristics [3]. However, a generalized equation to accommodate the air holes on an octagonal structure can be given as

$$(X_{Nn}, Y_{Nn}) = (N \times \Lambda \times \cos\theta_n , N \times \Lambda \times \sin\theta_n) \quad (4.11)$$

where θ_n represents the angle of rotation of air holes, N represents the total number of rings in the structure, Λ represents the pitch and n represents the number of air holes in a air hole ring where n=0.1.2.3.....(8N-1) and N=1...5. For example, in 1st ring, the number of air holes would be 8 and number of air holes in 2nd, 3rd, 4th, and 5th rings will be 16, 24, 32 and 40 respectively. Moreover the angle of rotation, θ_n for each air hole can be determined as

$$\theta_n = \frac{n\pi}{4N} \quad (4.12)$$

For example, the angle of rotation of 10 air hole of first ring (N=1) will be 0^0, whereas the angle of rotation of air holes from 11 to 17 (anticlockwise) will be $\frac{\pi}{4}$, $\frac{\pi}{2}, \frac{3\pi}{4}, \pi, \frac{5\pi}{4}, \frac{6\pi}{4}$ and $\frac{7\pi}{4}$ respectively. Furthermore, the radius of the air holes can be determined as same as the C-PCF using the Eq. (4.10).

4.4 Numerical simulation using COMSOL Multiphysics 4.2

COMSOL Multiphysics (formerly FEMLAB) 4.2 is a versatile simulation software based on FEM. It is a flexible platform that allows even novice users to model all relevant physical aspects of their designs. COMSOL Multiphysics also offers an extensive interface to MATLAB. Simulation of a DC-PCF model using COMSOL Multiphysics 4.2 software requires a high configuration computer. In this thesis, all simulations are

performed with a notebook of HP brand (ProBook 4440s). The detail configuration of used notebook is as follows

Table 2: Configuration of notebook

Processor	Intel core i5, 3230M CPU@2.60GHz
RAM (Installed)	8GB
OS	Windows 7, 64 bit
Cache memory RAM, (built into the processor)	3 MB

4.4.1 Simulation results of C-PCF

Fig. 4.4 shows the variation of chromatic dispersion against wavelength for the five rings C-PC. In our work, all the dispersion curves are presented only for fundamental mode and the optimum parameter of the proposed C-PCF is (Λ=1.0, d_1/Λ =0.95, d_2/Λ=0.81, d_3/Λ=0.98, d_4/Λ=0.60). From numerical simulation, it is found that the proposed dispersion compensating C-PCF shows large negative dispersion of about -248.65 to -1069 ps/(nm.km) for optimum parameter values in the wavelength range 1340-1640 nm (270 nm band). In particular, the negative dispersion at 1550 nm is -790.12 ps/(nm.km) and increases monotonically with decrease in Λ over the E to L wavelength bands ranging from 1360 to 1625 nm. Thus the proposed fiber can be used to compensate the accumulated dispersion of SMF currently deployed in WDM systems as it possesses large negative dispersion over a wide range of wavelength.

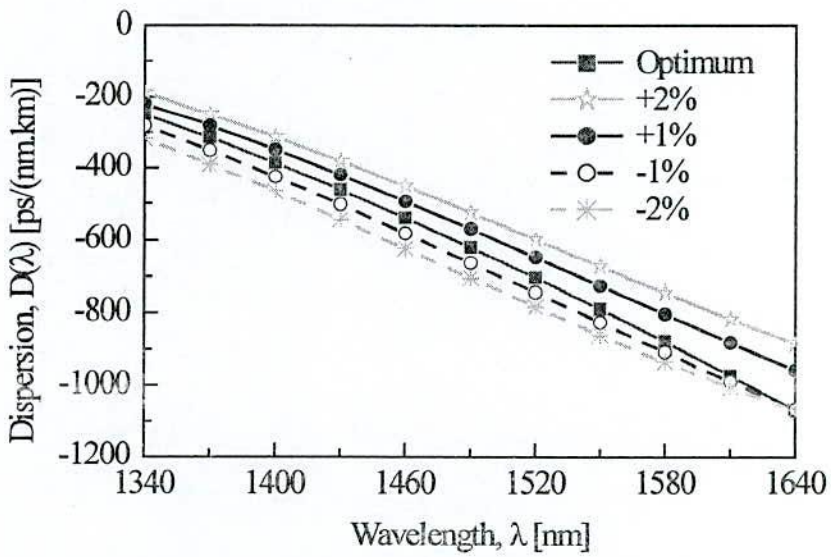

Fig. 4.4 Dispersion properties of C-PCF for fiber's global diameter variation.

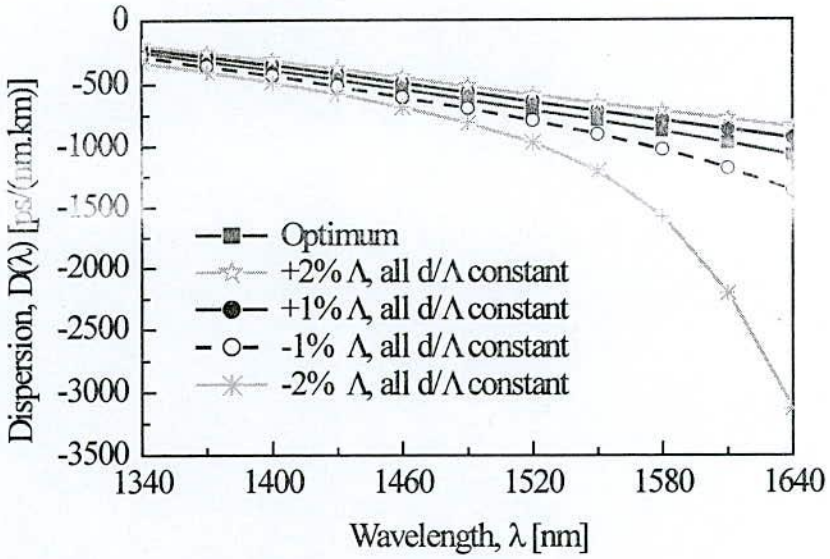

Fig. 4.5 Dispersion properties of C-PCF: optimum dispersion and effects of changing pitch Λ keeping all d/ Λ constant.

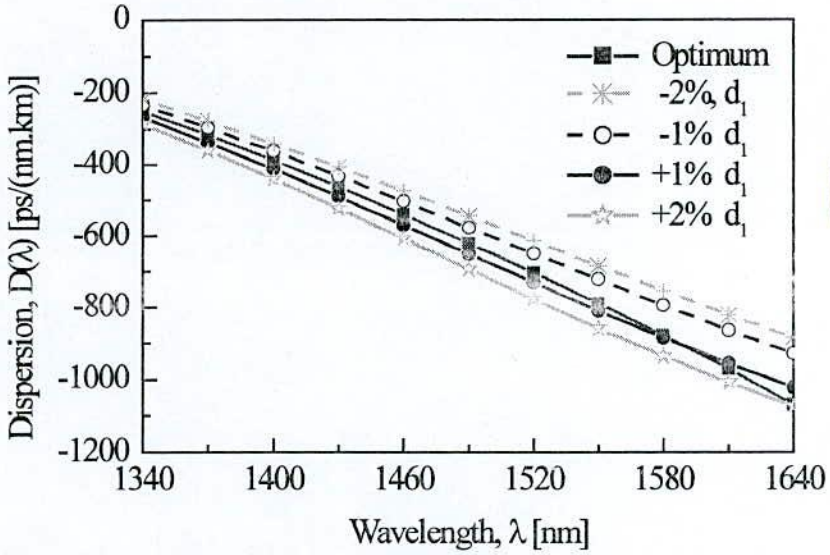

Fig. 4.6 Dispersion properties of C-PCF: optimum dispersion and effects of changing d_1.

Dispersion accuracy of the proposed fiber for variation in pitch, Λ while keeping all d/ Λ constant is shown in Fig. 4.5. It is found that the proposed C-PCF shows abrupt change in dispersion which occurs at 2% decrease in Λ. Figures 4.6, 4.7 and 4.8 show the dispersion properties of the proposed C-PCF for changing in diameters d_1, d_2 and d_3 respectively. It is obvious that the shape of dispersion curve is mostly dependent on the first air hole ring diameter, d_1. However, there is a little effect of changing outer diameters d_2 and d_4 on dispersion parameter and even variation in dispersion due to tuning d_2 and d_4 is found

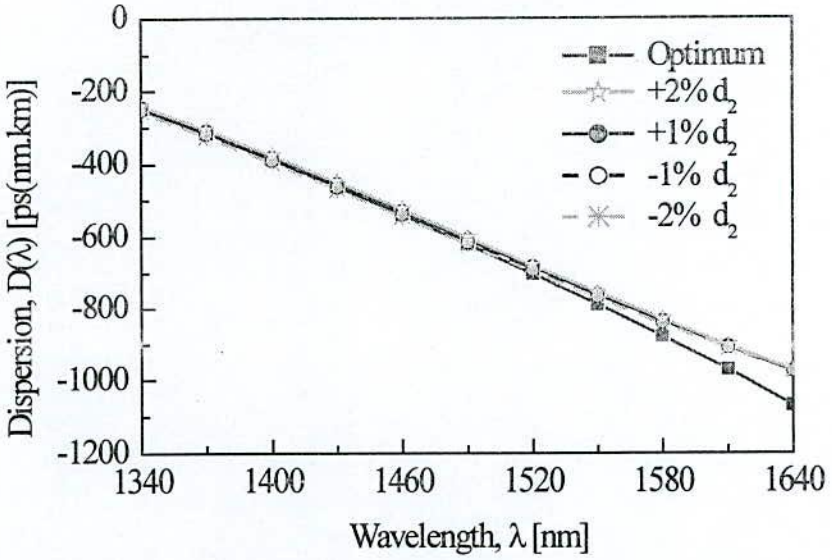

Fig. 4.7 Dispersion properties of C-PCF: optimum dispersion and effects of changing d_2.

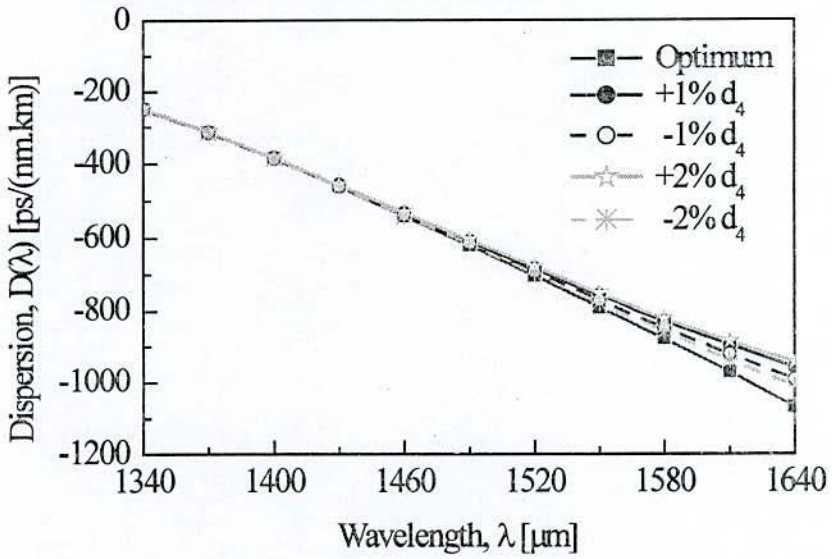

Fig. 4.8 Dispersion properties of C-PCF: optimum dispersion and effects of changing d_4.

negligible up to 1550 nm. Still, the negative dispersion coefficient is achieved higher for the optimum design parameters and it is significant in the wavelength higher than 1550 nm due to the variation of outer diameters d_2 and d_4. Relative dispersion slope, dispersion slope and effective dispersion are presented against wavelength for the proposed five rings C-PCF in Figures 4.9- 4.11 respectively. However, the RDS of the proposed fiber shown in Fig. 4.9 is obtained $0.0036\,nm^{-1}$ at 1550 nm wavelength which is perfectly matched with the SMF's RDS. It is observed that the variation in RDS is not significant over the entire band of interest which ensures that a small change in Λ will not affect the dispersion

slope compensation. Moreover, the dispersion slope curve possesses negative slope and variation in magnitude is less than that of which presented in [1]. Effective dispersion after compensating the positive dispersion of 40 km SMF by the proposed C-PCF for optimum parameters is shown in Fig. 4.11. It is to be mentioned here that the residual dispersion should be lower than ± 0.8 ps/(nm.km) [4] to compensate for a 40 Gbps signal. However, the maximum value of effective dispersion in usable bandwidth (1400-1600 nm) for the proposed C-PCF after compensating the dispersion of SMF is about ± 0.68 ps/(nm.km and particularly at 1550 and 1430 nm, effective dispersion is zero.

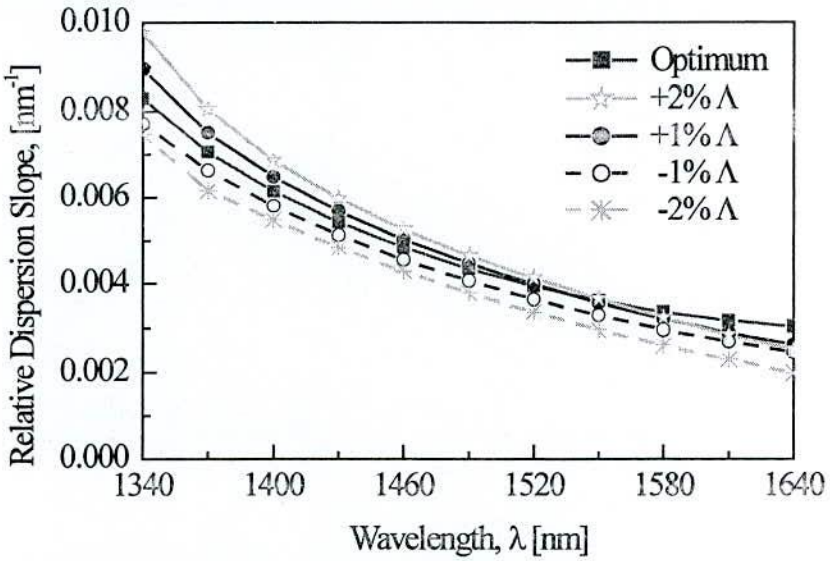

Fig. 4.9 Effect of changing pitch, Λ on residual dispersion slope.

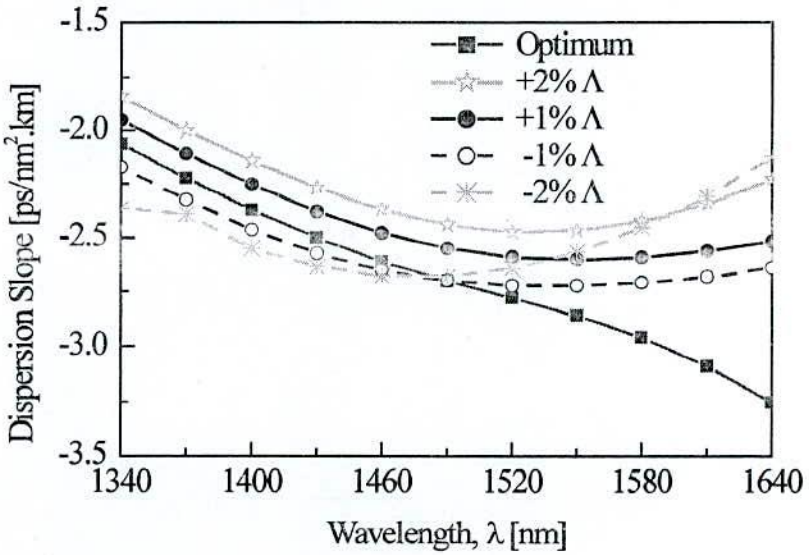

Fig. 4.10 Dispersion slope of C-PCF showing the effects of changing Λ.

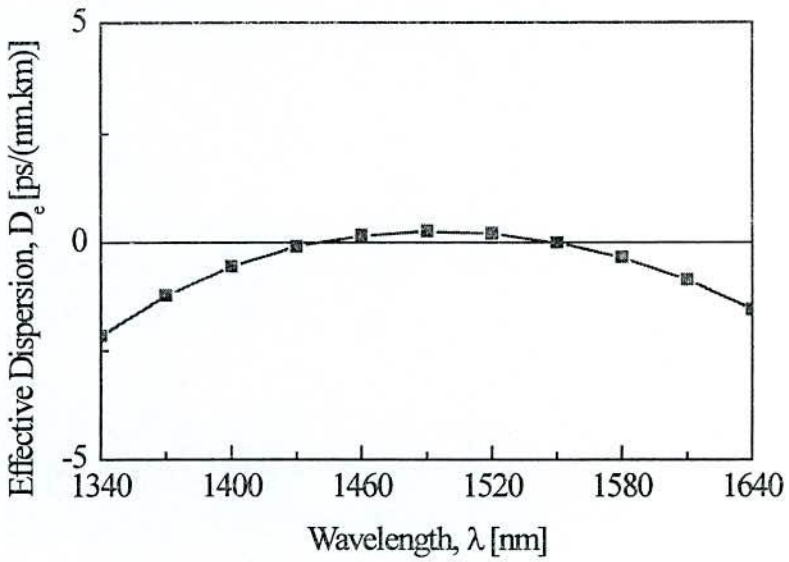

Fig. 4.11 Variation of effective dispersion against wavelength of 818.4 m long optimized C-PCF to compensate for a 40 km long standard SMFs.

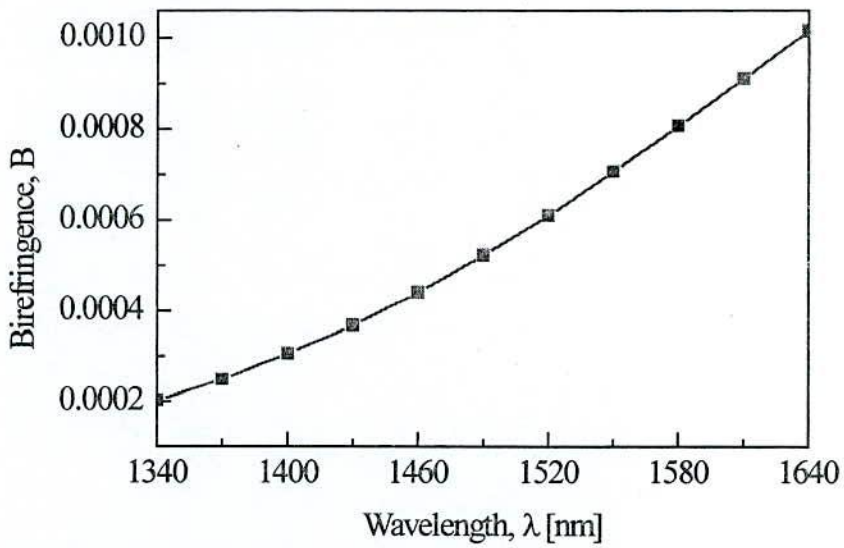

Fig. 4.12 Birefringence property of the proposed C-PCF for the optimum design parameters: $\Lambda=1.0$, $d_1/\Lambda=0.95$, $d_2/\Lambda=0.81$, $d_3/\Lambda=0.98$, $d_4/\Lambda=0.60$.

Thus, it is clearly understood that our proposed C-PCF with optimized parameters is suitable for systems with high bit rates transmission systems covering entire S- and C-band effectively and even some portion of the L band. Besides, our proposed C-PCF exhibits a modal birefringence of about 7×10^{-4} at 1550 nm as shown in Fig. 4.12. However, this value of birefringence is not enough to eliminate the effect of PMD. As a result, the proposed C-PCF although capable enough to compensate broadband dispersion

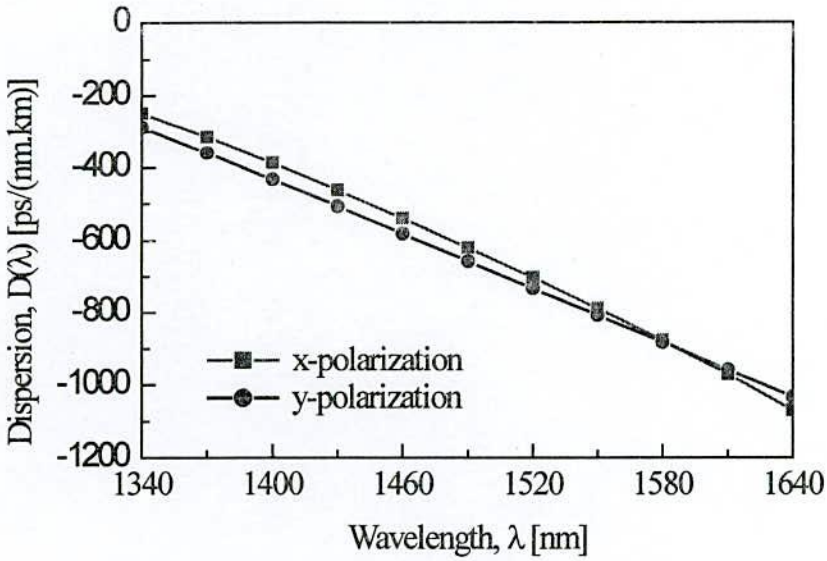

Fig. 4.13 Wavelength response of chromatic dispersion of the proposed C-PCF for both x- and y-polarization for the optimum design parameters.

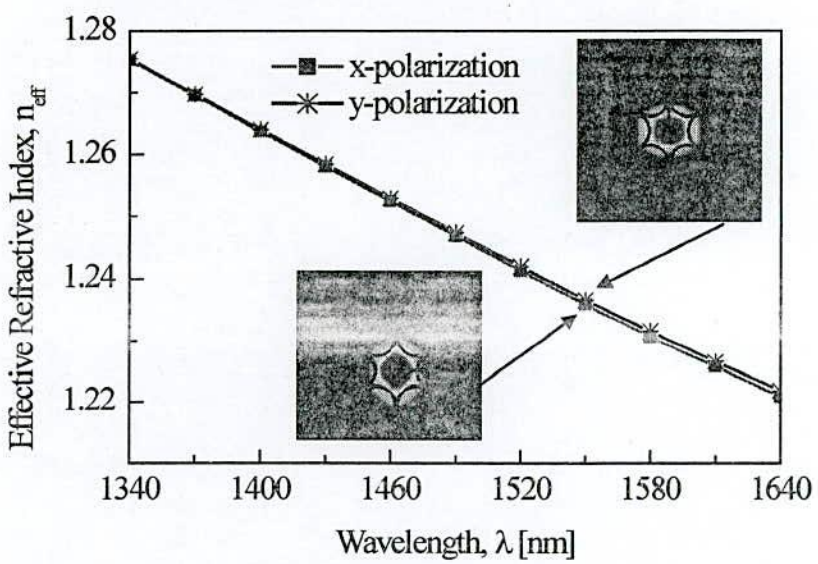

Fig. 4.14 Variation in the effective refractive index for both x- and y-polarization for the optimized C-PCF.

but still suffers from the PMD in transmission system. In addition, it will not be suitable for some other areas where PM properties are essentially required such as sensing applications. Chromatic dispersion of both polarization states is shown in Fig. 4.13. Effective refractive index of both x- and y-polarization is presented in Fig. 4.14 where the insets are electric field distributions at $\lambda = 1550$ nm for each polarization state. Fig. 4.15 represents the effective area of the proposed five rings C-PCF which increases with

wavelength for optimum design parameters and also for fiber's global diameter variation. In particular, the effective area at λ=1550 nm is 1.574 μm^2 for the optimum parameters which is higher than that obtained for eight ring DC-MOF [6] but lower than [7]. However, low effective area causes splice loss and as a solution, tapered intermediate PCF can be used for interfacing between proposed C-PCF and SMF successfully [8]. So, we believe that our proposed C-PCF can be interconnected with SMF without any major complications.

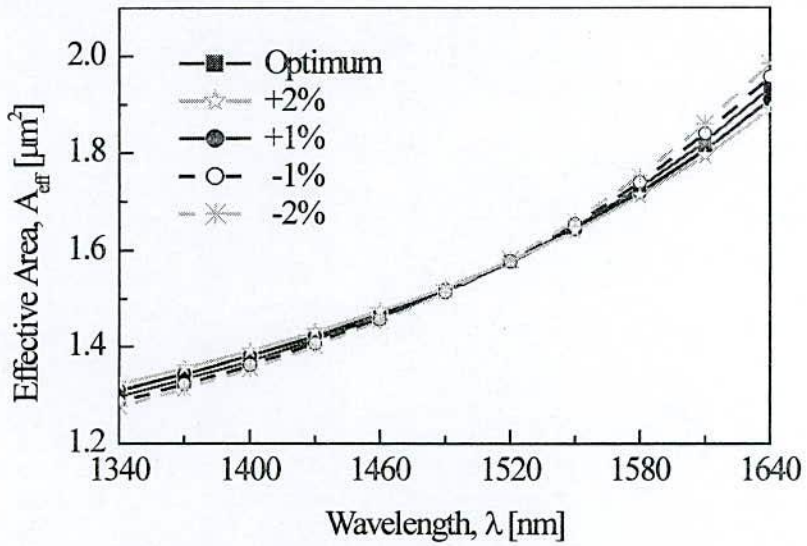

Fig. 4.15 Effective area of the proposed C-PCF for optimum design parameters and also for fiber's global diameter variations of order ±1 to ±2% around the optimum value.

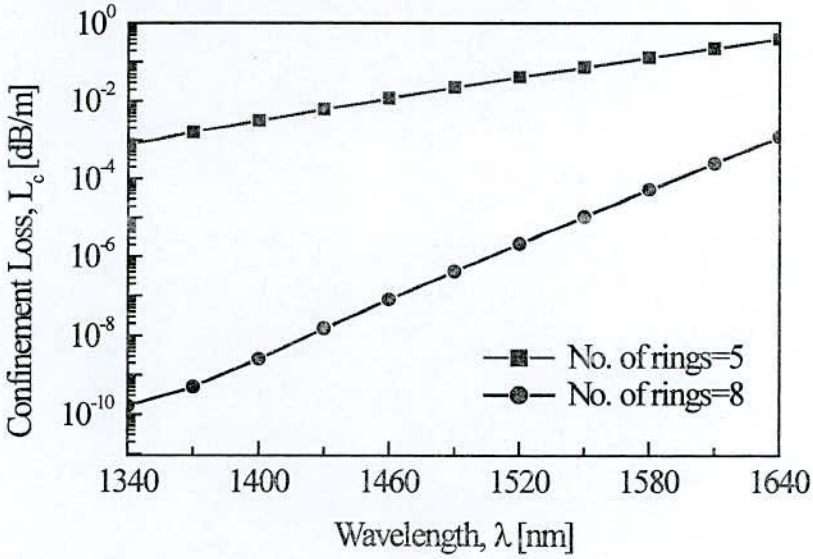

Fig. 4.16 Confinement loss of the proposed C-PCF for the optimum parameters and also showing the effect of increasing number of rings on confinement loss.

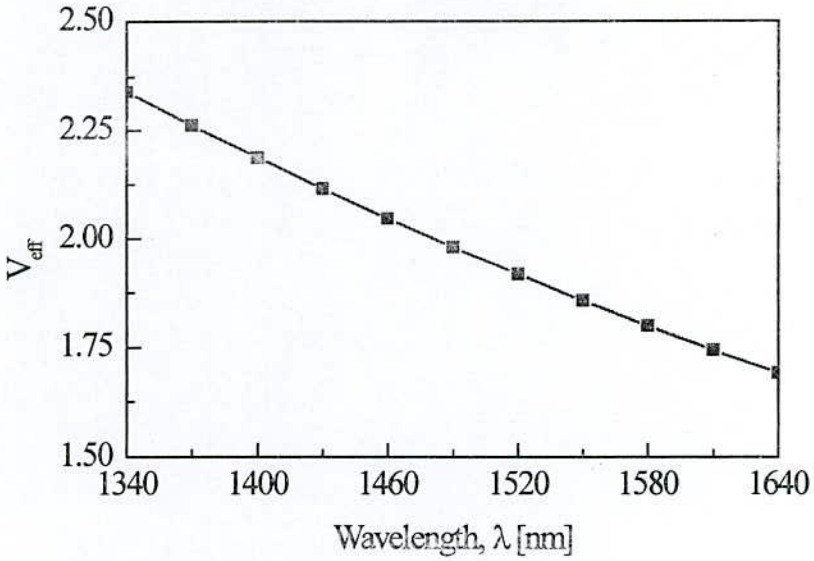

Fig. 4.17 Variation of effective V-parameter of the proposed C-PCF for optimum design parameters.

Fig. 4.16 describes the wavelength dependence properties of the confinement loss of the proposed C-PCF. Confinement loss only for optimum parameters is shown for both five rings and eight rings. From figure, it is observed that the confinement loss is about 0.073587 and 1.0637×10^{-5}dB/m at λ=1550 nm for five and eight air-hole rings respectively which are the acceptable level for the transmission fiber. It should be noted that the numbers of rings mostly control the confinement loss and reduces significantly with the increase of rings. However 20, 11, 13 and 9 air hole rings are considered by [9-10,11,1] to keep the confinement loss below 10^{-4} dB/m to cover S band [11], C band [9] and wavelength ranging from 1.46 to 1.64 μm [1, 10]. Therefore, the design complexity of the proposed C-PCF is lower than mentioned above in terms of number of rings used. The effective V-parameter, V_{eff} for the proposed C-PCF has been presented in Fig. 4.17 for the entire band of interest ranging from 1340-1640 nm wavelengths. However, simulation results show that the maximum value of V_{eff} is 2.3402 at 1340 nm and obviously the presented figure satisfies the condition $V_{eff} < \pi$ for the entire band of interest. Thus, our proposed C-PCF will support only a single mode rather than multimode within that range of wavelength.

4.4.2 Simulation results of M-CPCF

Fig. 4.18 shows the variation of chromatic dispersion against wavelength of the five rings M-CPCF for fundamental mode for optimum design parameters (Λ=1.0, d_1/Λ =0.95, d_2/Λ=0.70, d_3/Λ =0.60, η=0.22) and also for variation of Λ. Simulation result also reveals that it is possible to obtain large negative dispersion coefficient of -203.8 to -835.14 ps/(nm.km) using the proposed dispersion compensating M-CPCF for optimum parameter values against wavelength ranging from 1340-1640 nm (270 nm band). In particular, the negative dispersion at 1550 nm is -643.62 ps/(nm.km) for the five rings M-CPCF which is less than what obtained at 1550 nm for C-PCF. However, the negative dispersion coefficient still increases monotonically with decrease in Λ and thus possesses negative dispersion slope over the entire band of interest providing good dispersion compensating ability. Thus, the proposed fiber can be used to compensate accumulated dispersion of SMF currently deployed in WDM systems as it possesses large negative dispersion over a wide range of wavelength. Dispersion properties of the proposed M-CPCF for tuning only Λ keeping all d/Λ constant has been shown in Fig. 4.19. It is observed clearly that the negative dispersion coefficient increases smoothly with decrease in Λ without any abrupt change in dispersion coefficient which provides better dispersion accuracy. Figures 4.20-4.22 illustrate the dispersion accuracy of the proposed M-CPCF against wavelength for varying air hole diameters. Dispersion accuracy with the variation of air hole diameter, d_1 has been shown in Fig. 4.20. It is found that the negative dispersion coefficient is increased with increase in d_1.

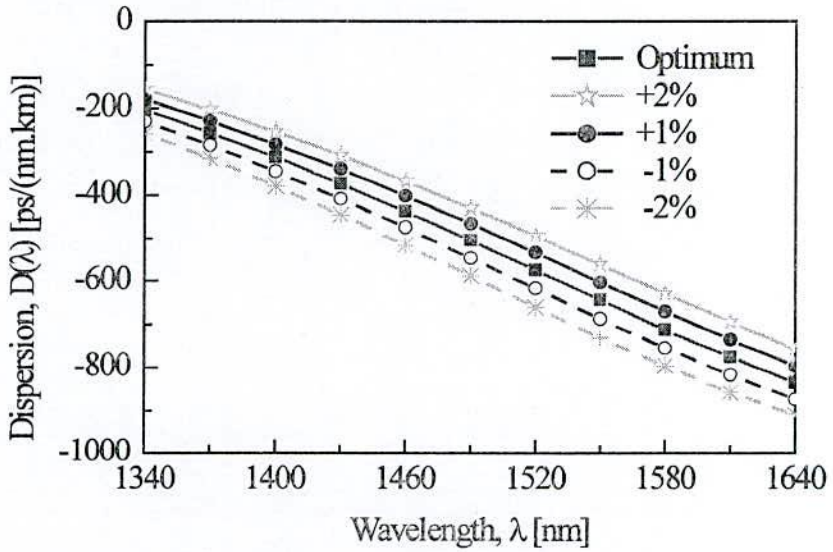

Fig. 4.18 Dispersion properties of M-CPCF for fiber's global diameter variation.

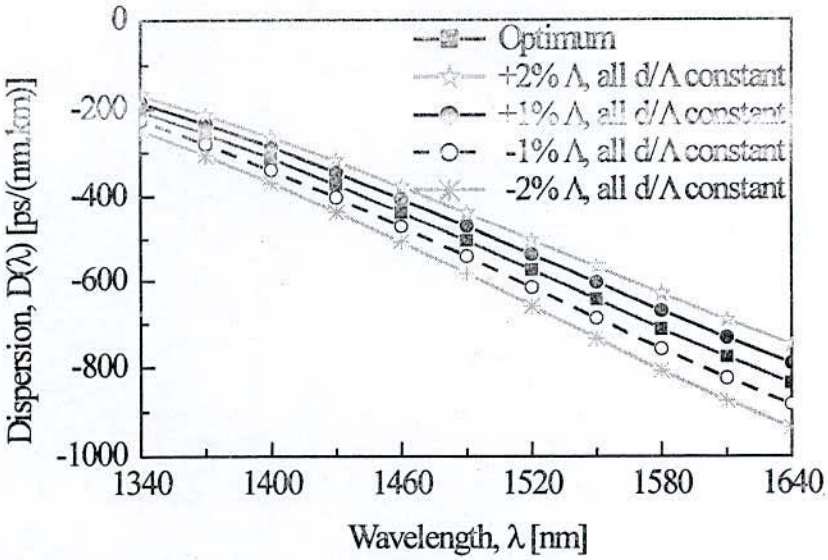

Fig. 4.19 Dispersion properties of M-CPCF: optimum dispersion and effects of changing pitch Λ keeping all d/Λ constant.

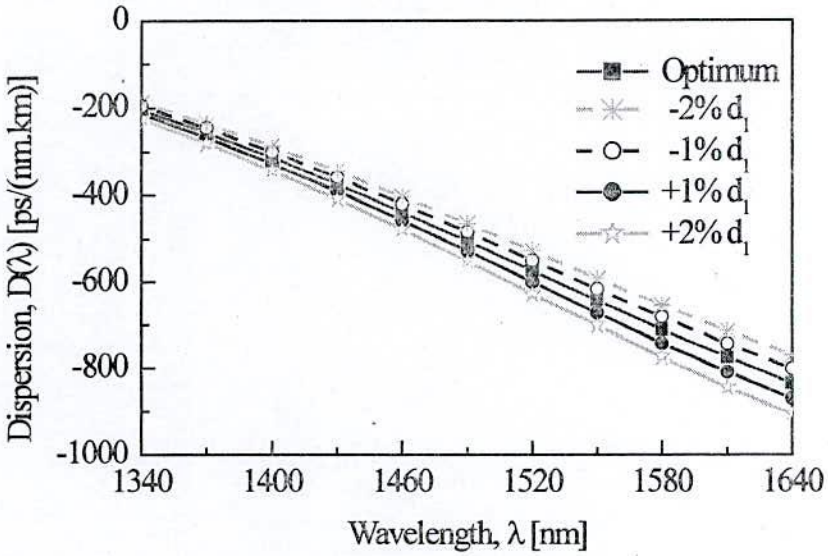

Fig. 4.20 Dispersion properties of M-CPCF: optimum dispersion and effects of tuning, d_1.

However, the change in negative dispersion coefficient for tuning the diameters d_2 and d_3 are shown in Fig. 4.21 and 4.22 respectively. The change in negative dispersion from optimum value is not significant due to the variation of d_2 and remains almost same due to changing d_3 over the wavelength band ranging from 1340-1640 nm. Hence air hole diameter, d_1 mostly controls the negative dispersion coefficient. Fig. 4.23 shows the residual dispersion slope of the proposed M-CPCF for optimum parameters and due to the

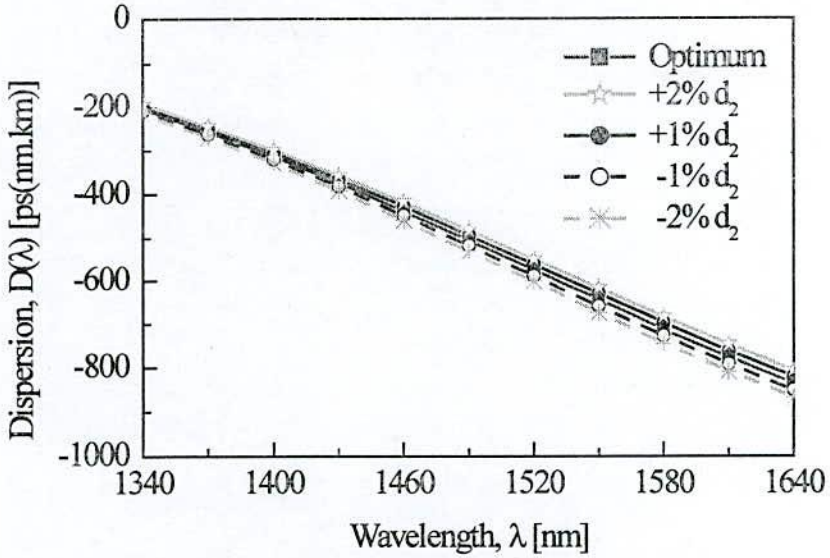

Fig. 4.21 Dispersion properties of M-CPCF: optimum dispersion and effects of tuning, d_2.

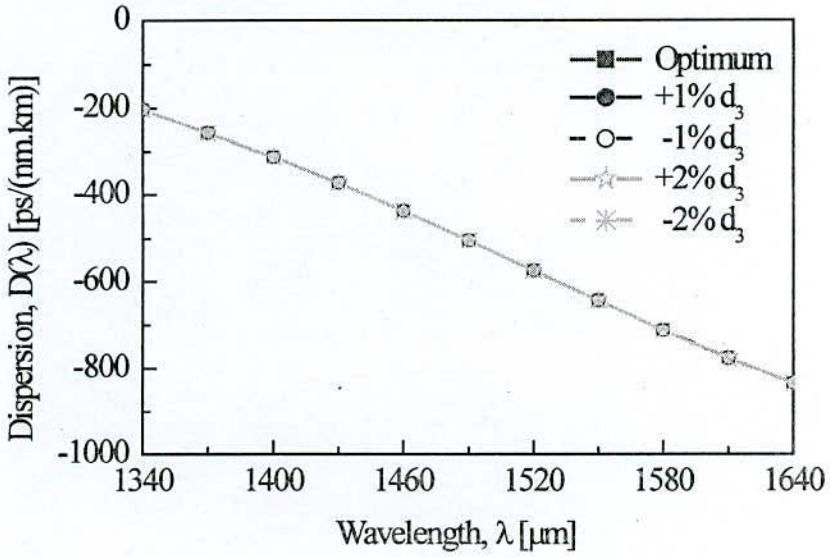

Fig. 4.22 Dispersion properties of M-CPCF: optimum dispersion and effects of tuning, d_3.

variation of pitch, Λ. For optimum design parameters, the relative dispersion slope of the proposed M-CPCF is exactly equal to the relative dispersion slope of SMF of about 0.0036 nm^{-1} at 1550 nm wavelength. Thus, the requirement of slope compensation is fulfilled. However, relative dispersion slope increases smoothly with increase in Λ but deviation from the optimum value is not noteworthy. The dispersion slope of the proposed M-CPCF has been illustrated in Fig. 4.24. It is clearly observed from the figure that it possesses the negative dispersion slope over the wavelength band ranging from 1340 to 1640 nm and thus complies with the requirement of broadband dispersion compensation. Moreover, the

variation in dispersion slope is low and even negligible particularly at 1580 nm wavelength. Fig. 4.25 shows the variation of effective dispersion against wavelength of 1.15 km long optimized M-CPCF to compensate for a 40 km long standard SMFs. However, the effective dispersion of the proposed M-CPCF is zero at 1430 and 1550 nm respectively and it is within ± 0.8 ps/(nm.km) form 1360 to 1640 nm. Thus, it is seen that the optimized M-CPCF is capable of compensating dispersion over E ot L

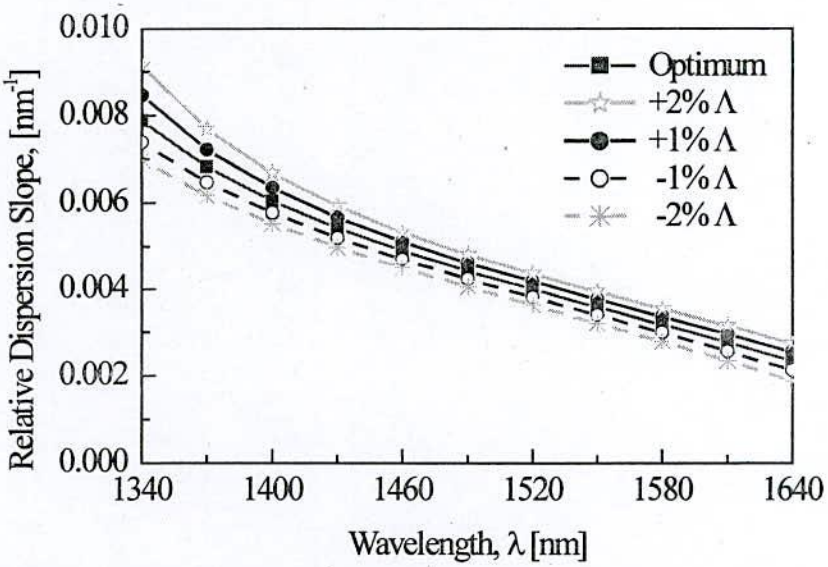

Fig. 4.23 Effect of pitch, Λ on residual dispersion slope of the proposed M-CPCF.

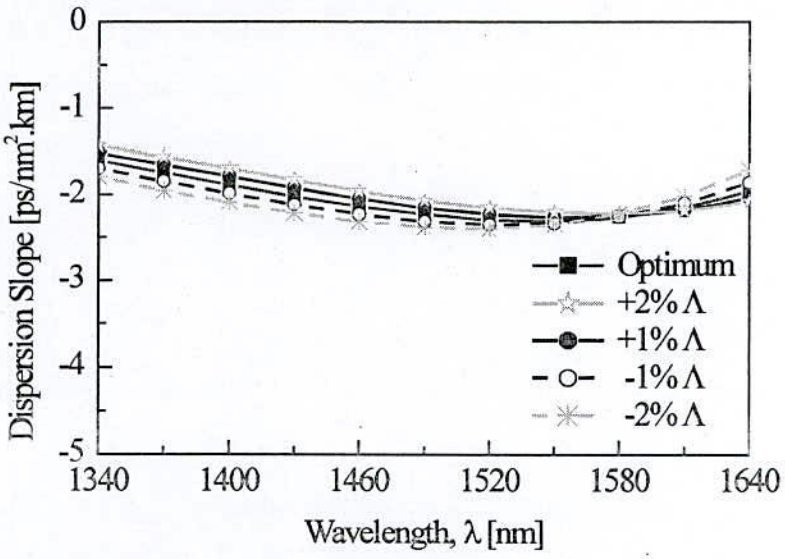

Fig. 4.24 Dispersion slope of M-CPCF showing the effects of Λ.

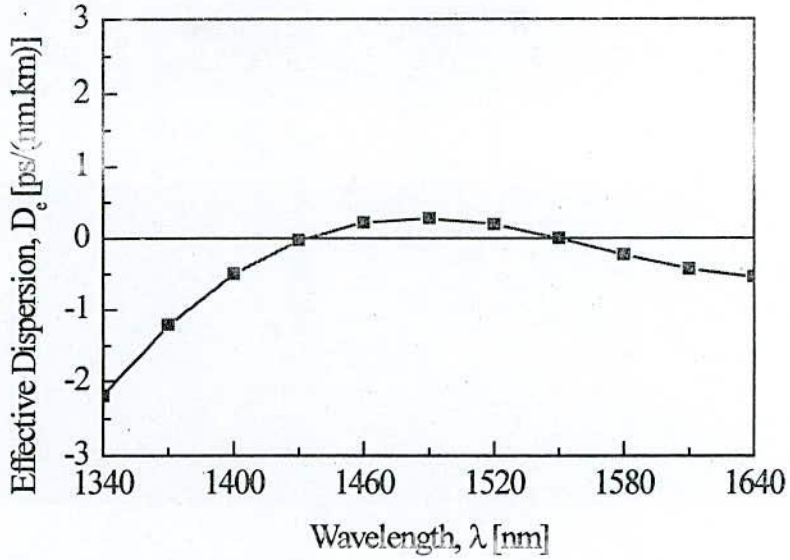

Fig. 4.25 Variation of effective dispersion against wavelength of 1.15 km long optimized M-CPCF to compensate for a 40 km long standard SMFs.

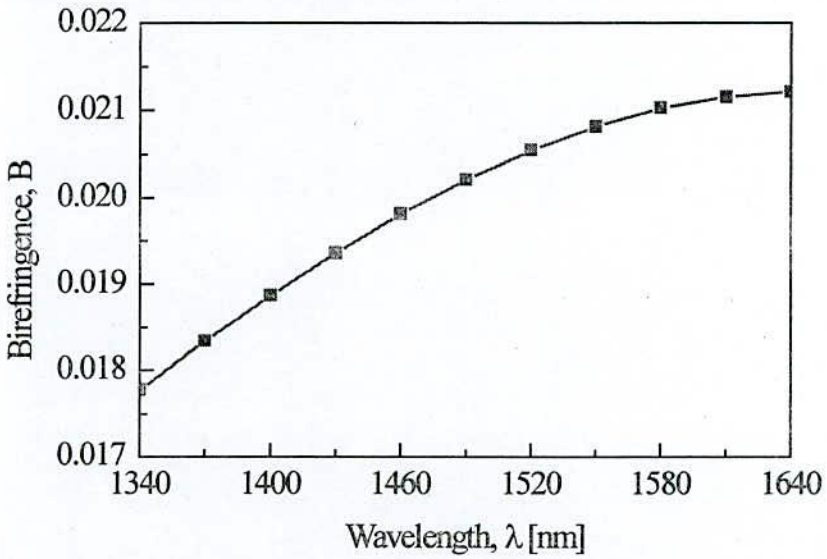

Fig. 4.26 Birefringence property of the proposed M-CPCF for the optimum design parameters: $\Lambda=1.0$, $d_1/\Lambda=0.95$, $d_2/\Lambda=0.70$, $d_3/\Lambda=0.60$, $\eta=0.22$.

telecommunication band ranging from 1360 to 1620 nm and expected to compensate the dispersion up to U band (1675 nm) caused by standard SMFs. The birefringence property of the proposed M-CPCF has been presented in Fig. 4.26 which shows high birefringence of about 2.2×10^{-2} at 1550 nm and increases with wavelength. Hence, the beat length of the proposed fiber will be small which will maintain a single polarization state thus eliminates the effect of PMD. Fig. 4.27 illustrates the effective refractive index of the two orthogonal

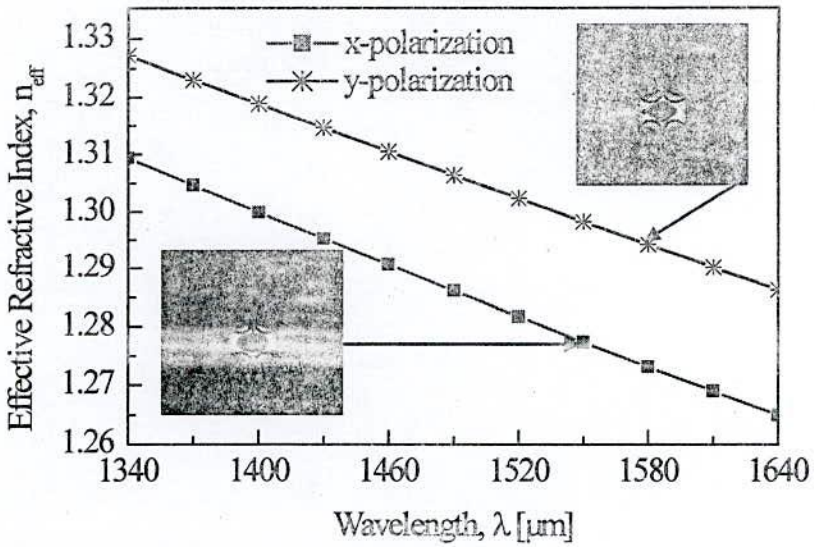

Fig. 4.27 Wavelength dependent response of effective refractive index of the proposed M-CPCF for both x- and y-polarization for the optimum design parameters.

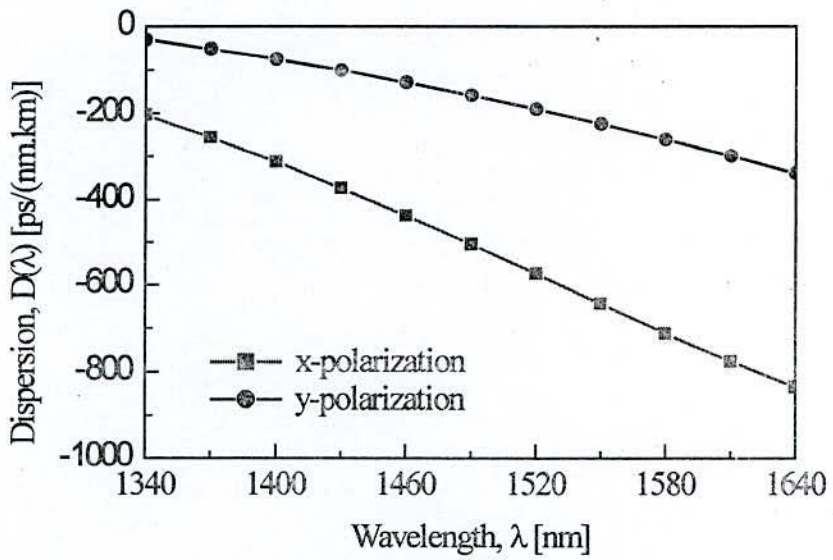

Fig. 4.28 Wavelength response of chromatic dispersion of the proposed M-CPCF for both x- and y-polarization for the optimum design parameters.

polarization axis which shows a significant difference in refractive index between these two orthogonal axis. Moreover, the insets represent the electric field distributions at λ = 1550 nm for each polarization state. However, wavelength dependence chromatic dispersion for two orthogonal polarization states is shown in Fig. 4.28. It is clearly shows that the difference in chromatic dispersion is high and increasing with increase in wavelength. Hence, it is expected that the proposed fiber will have the polarization

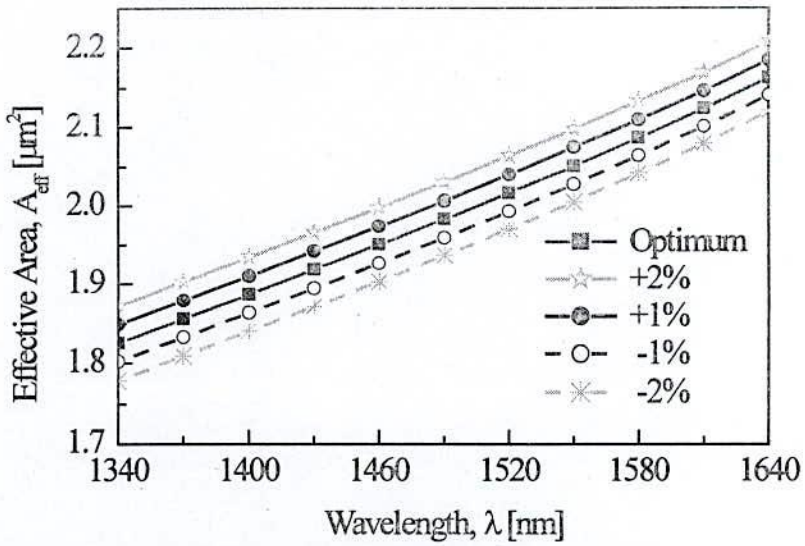

Fig. 4.29 Effective area of the proposed M-CPCF for optimum design parameters and also for fiber's global diameter variations of order ±1 to ±2% around the optimum value.

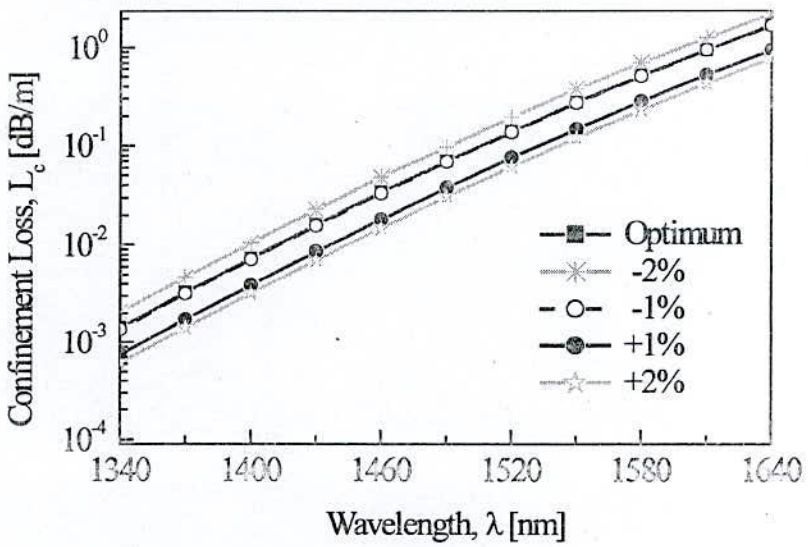

Fig. 4.30 Confinement loss of the proposed M-CPCF for the optimum parameters and also for fiber's global diameter variations of order ±1 to ±2% around the optimum value.

maintaining capability and will maintain a single polarization state. Fig 4.29 shows the variation of effective area with wavelength for optimum parameters and fiber's global diameter variation up to ±2%. The effective area of the proposed fiber is about 2.05 μm^2 at 1550 nm wavelength. However, the effective area is increasing with increase in wavelength and Λ. Moreover, the effective area of the M-CPCF is not even enough but still greater than that obtained for the C-PCF. Fig. 4.30 shows the confinement of the

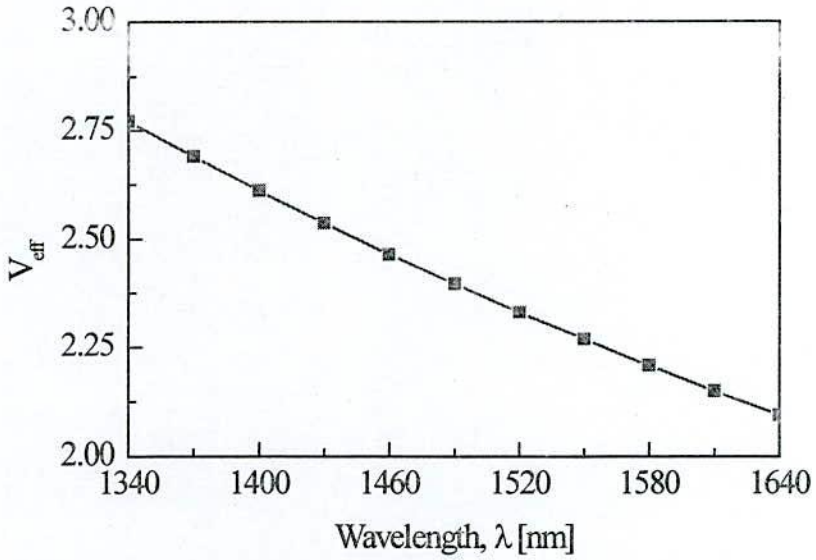

Fig. 4.31 Variation of effective V-parameter for the optimized M-CPCF.

proposed M-CPCF. It is observed from the figure that the confinement loss is increased due to increasing the pitch, Λ. The effective V-parameter has been shown in Fig. 4.31. From the figure, it is clear that all values of $V_{eff} < \pi$ and thus the proposed M-CPCF will only support single mode rather multimode.

4.4.3 Simulation results of M-OPCF

Fig. 4.32 shows wavelength response of chromatic dispersion of the proposed M-OPCF for optimum design parameters ($d_1/\Lambda = 0.73$, $d_2/\Lambda = 0.53$, $d_3/\Lambda = 0.70$, and $\eta = 0.307$) and the fiber's global diameter variation up to ±2% from the optimum value. It can be seen that for the optimized set of parameters and air-hole configurations (η, Λ, d_1, d_2, and d_3), a large negative dispersion coefficient of about −470 to −850 ps/(nm.km) can be obtained which is monotonically increases over S to L-bands wavelength ranging from 1460 to 1625 nm and consequently possesses negative dispersion slope, providing fine dispersion compensation. Fig. 4.33 illustrates the effect of changing the pitch, Λ on dispersion, while the rest of the geometrical parameters are kept constant. This figure ensures that design accuracy of the fiber up to ±1% change in the pitch is within ±53 ps/nm/km maintaining desired dispersion characteristics. From the above results, it is clear that a large negative dispersion is obtained and the dispersion value of the proposed M-OPCF at 1550 nm wavelength is about −672 ps/nm/km which is higher than [4] and far exceeding the

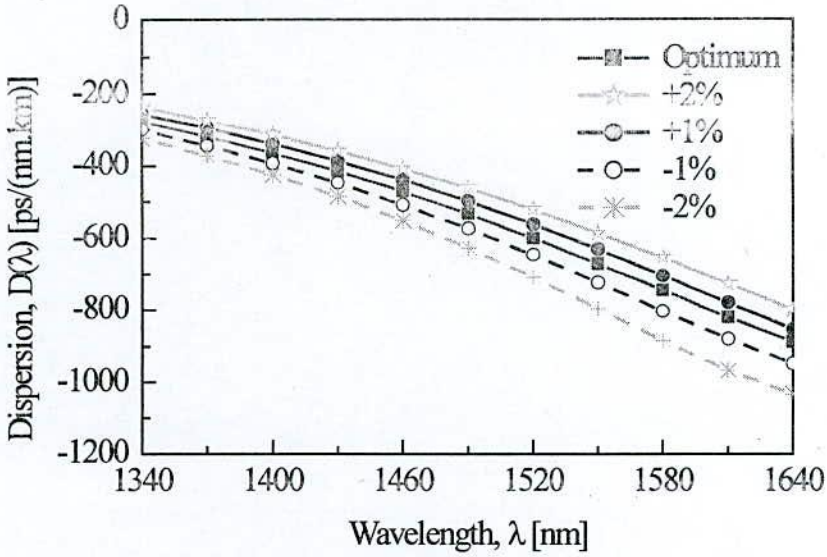

Fig. 4.32 Dispersion properties of M-OPCF: optimum dispersion and dispersion due to fiber's global diameter variation.

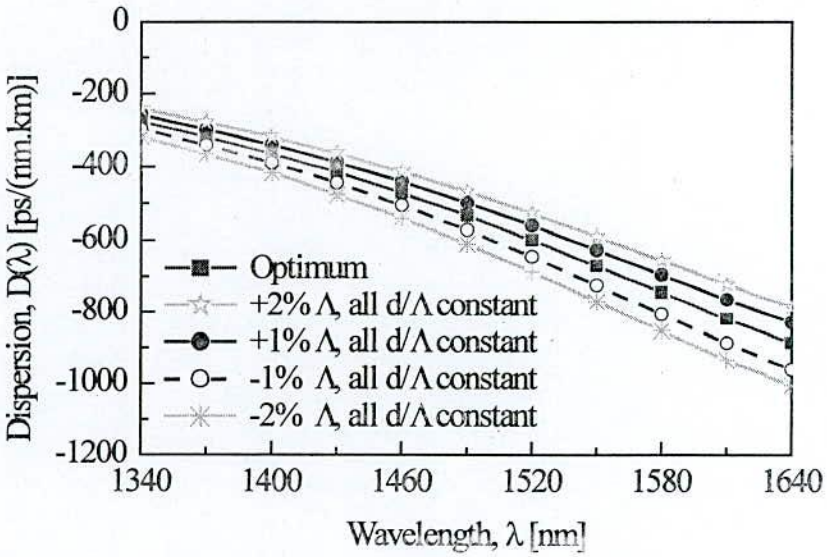

Fig. 4.33 Dispersion properties of M-OPCF: optimum dispersion and effects of changing pitch Λ keeping all d/Λ constant.

dispersion values of conventional dispersion compensating fibers which is typically −100 ps/(nm.km) [12]. We have also checked the dispersion accuracy of the proposed fiber because in a standard fiber draw, ±2% variations in fiber global diameter may occur [13] during the fabrication process. Therefore, roughly an accuracy of ±2% may require ensuring dispersion tolerance [14]. To account for this structural variation, diameter of

first and second air-hole ring, d_1 is varied up to ±2% from their optimum values while keeping other fiber parameters fixed. Fig. 4.34 shows the effect of variation of air-hole diameter, d_1 on dispersion curve. It can be examined that the dispersion shifts to down/up direction with increase/decrease in the d_1. It is found that the proposed M-OPCF maintains dispersion within a ±50 ps/(nm.km) for variations of d_1 up to ±2% at 1550 nm. Therefore, it can be concluded that ±2% change d_1 doesn't affect the performances of the device drastically.

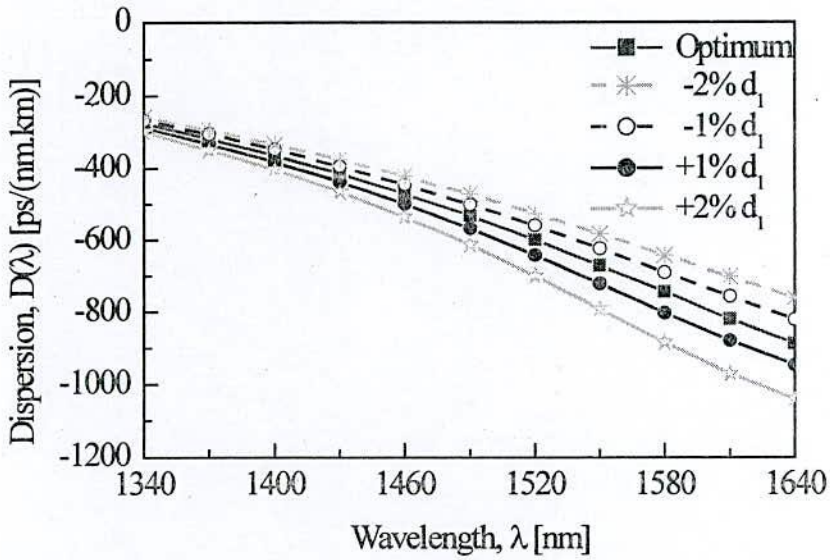

Fig. 4.34 Dispersion properties of M-OPCF: optimum dispersion and effects of tuning, d_1.

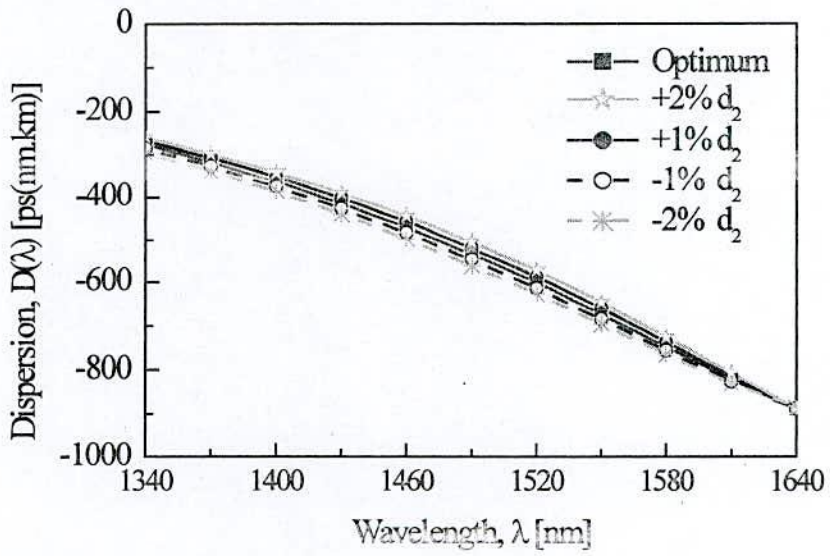

Fig. 4.35 Dispersion properties of M-OPCF: optimum dispersion and effects of tuning, d_2.

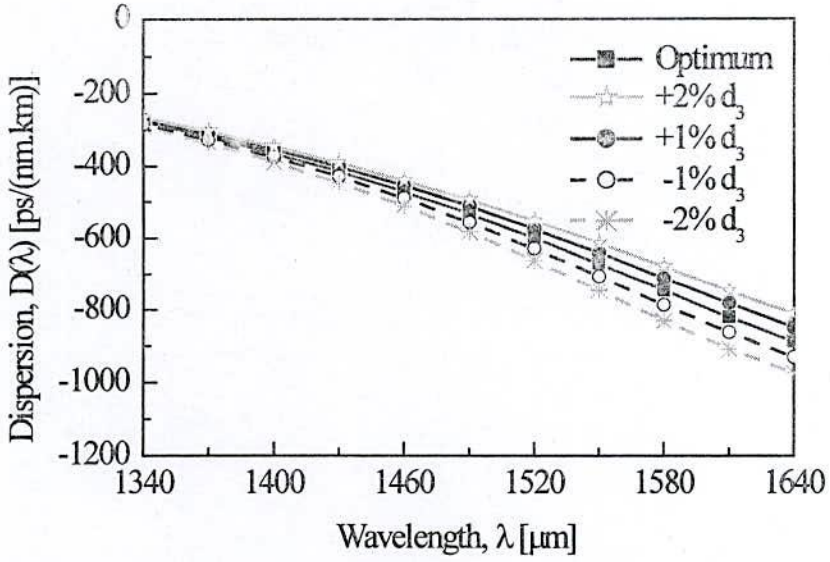

Fig. 4.36 Dispersion properties of M-OPCF: optimum dispersion and effects of tuning, d_3.

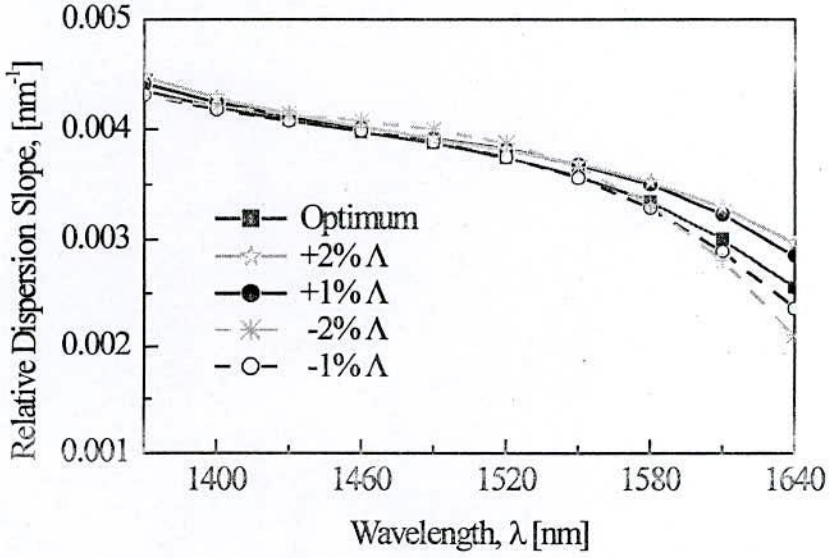

Fig. 4.37 Effect of pitch, Λ on residual dispersion slope of the proposed M-OPCF.

As a next step, we have analyzed the effect of changing d_2 on dispersion behavior. Fig. 4.35 shows the effect of changing the third air-hole ring diameter, d_2 on dispersion, while the rest of the geometrical parameters are kept constant. This figure ensures that design accuracy of the fiber up to ±1% change in the pitch is within ±14 ps/nm/km maintaining desired dispersion characteristics. Next, we have also checked the impact of d_3 on dispersion. Fig. 4.36 shows the effect of changing the fourth and fifth air-hole ring diameter, d_3 on dispersion, while the rest of the geometrical parameters are kept constant. This figure ensures that design accuracy of the fiber up to ±1% change in pitch is within

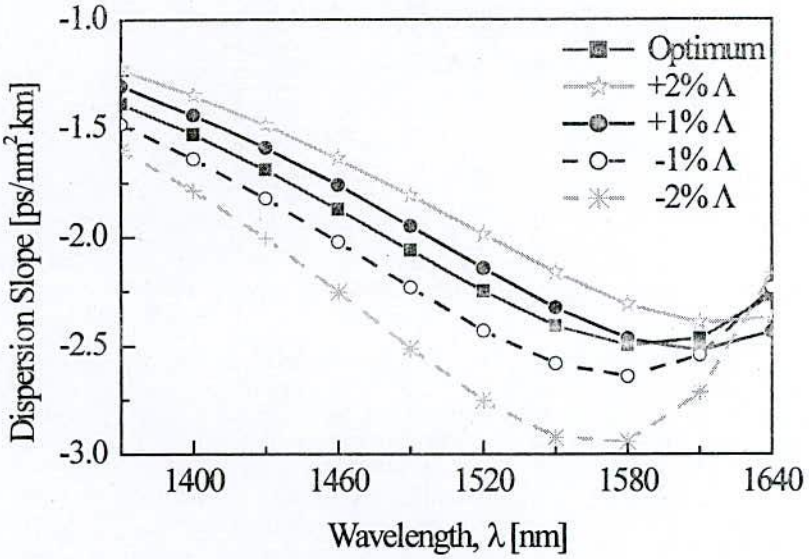

Fig. 4.38 Effect of pitch, Λ on dispersion slope of the proposed M-OPCF.

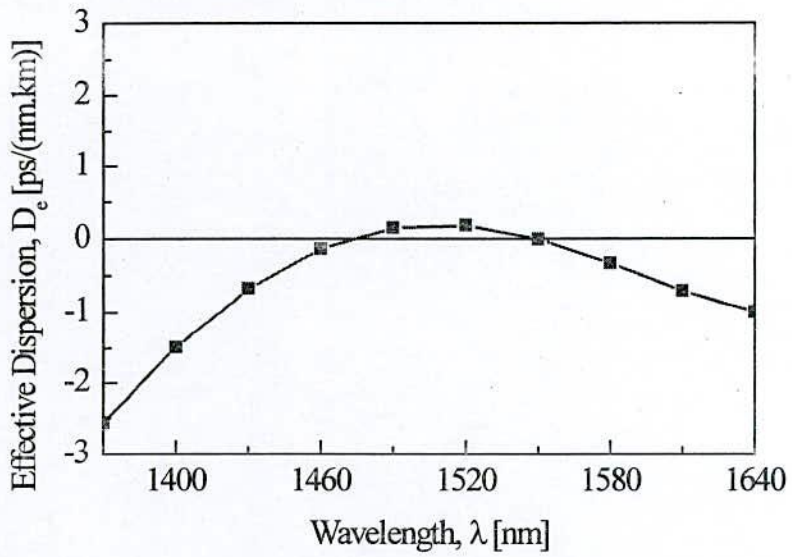

Fig. 4.39 Variation of effective dispersion against wavelength of 1.10 km long optimized M-OPCF to compensate for a 40 km long standard SMFs.

±20 ps/nm/km maintaining desired dispersion characteristics. Relative dispersion slope curve has been presented in Fig. 4.37. For optimum design parameter, the relative dispersion slope of the proposed M-OPCF is exactly equal to the relative dispersion slope of SMF of about 0.0036 nm^{-1} at 1550 nm wavelength. Thus, the requirement of slope compensation is satisfied. However, relative dispersion slope increases smoothly with increase in Λ but deviation from the optimum value is not noteworthy. The dispersion slope of the proposed M-OPCF has been

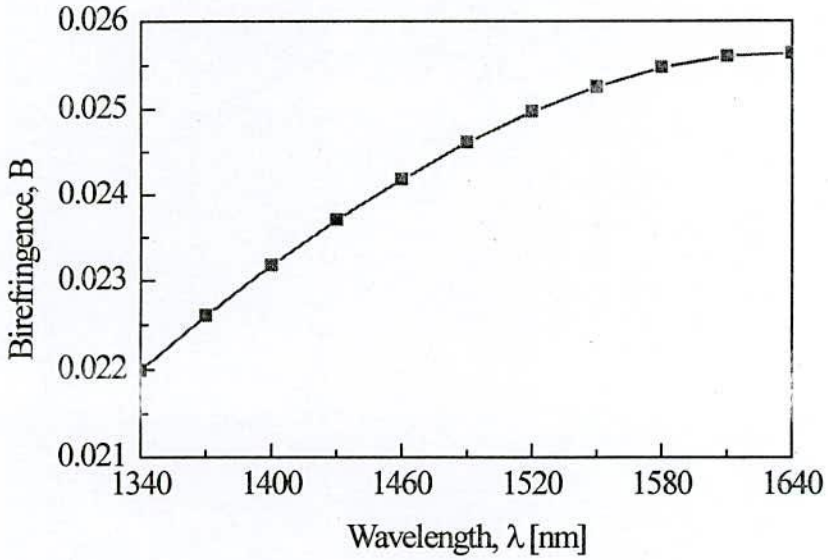

Fig. 4.40 Birefringence property of the proposed M-OPCF for the optimum design parameters: $d_1/\Lambda = 0.73$, $d_2/\Lambda = 0.53$, $d_3/\Lambda = 0.70$, and $\eta = 0.307$.

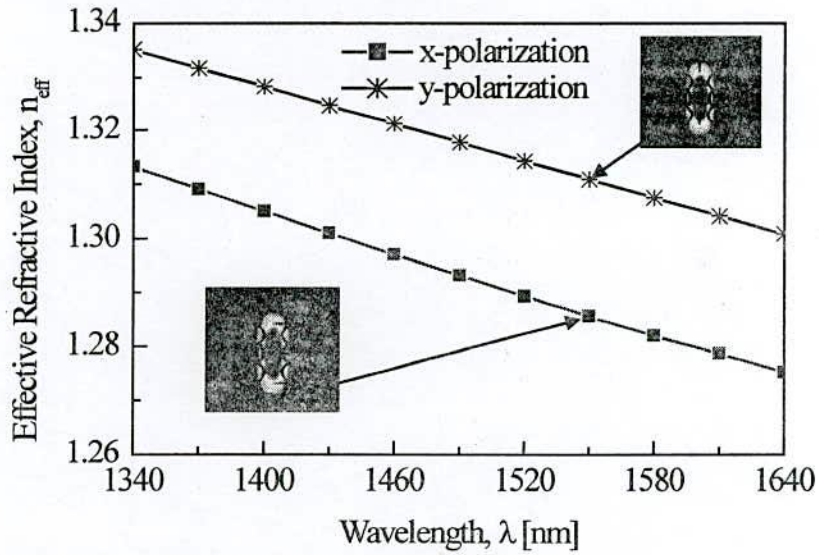

Fig. 4.41 Wavelength dependent response of effective refractive index of the proposed M-OPCF for both x- and y-polarization for the optimum design parameters.

illustrated in Fig. 4.38. It is clearly observed from the figure that it possesses the negative dispersion slope over the wavelength band ranging from 1340 to 1640 nm and thus complies with the requirement of broadband dispersion compensation. Fig. 4.39 corresponds effective dispersion obtained after the dispersion compensation by 1.10 km long M-OPCF for the dispersion accumulated in one span (40 km) of SMF for the optimum design parameters. From the figure, effective dispersion is found within ±0.6

ps/(nm.km) range and thus, it is clearly proved that our proposed M-OPCF with optimized parameters is suitable for systems with high bit rates 40Gb/s covering S to L communication bands. Fig. 4.40 shows the wavelength response of birefringence property for the optimum design parameters. The optimum design parameters give a value of birefringence of 2.53×10^{-2} at 1550 nm wavelength which is a very high value, two orders of magnitude higher than that of conventional PM fibers [15]. In this case, the corresponding beat length is 0.061mm at 1550 nm wavelength which is lower than [4, 16]. This shows that the proposed M-OPCF is highly birefringent. Also, a high birefringence fiber could be very useful in a polarization maintaining transmission system [17] and can be used to eliminate the effect of PMD in transmission systems. Therefore, the proposed M-OPCF could be a potential candidate for optical fiber sensing and polarization maintaining transmission system. Fig. 4.41 shows effective refractive indices for the orthogonal axis of the proposed M-OPCF with their respective fundamental electric field properties at λ = 1550 nm. It is found that the effective refractive index of the y-polarization is higher than that of the x-polarization. However, the difference in refractive index provides a high birefringence on the order of 10^{-2}. The asymmetrical design of the core of the proposed M-OPCF causes a considerable increase in linear birefringence properties, which is suitable for PM applications.

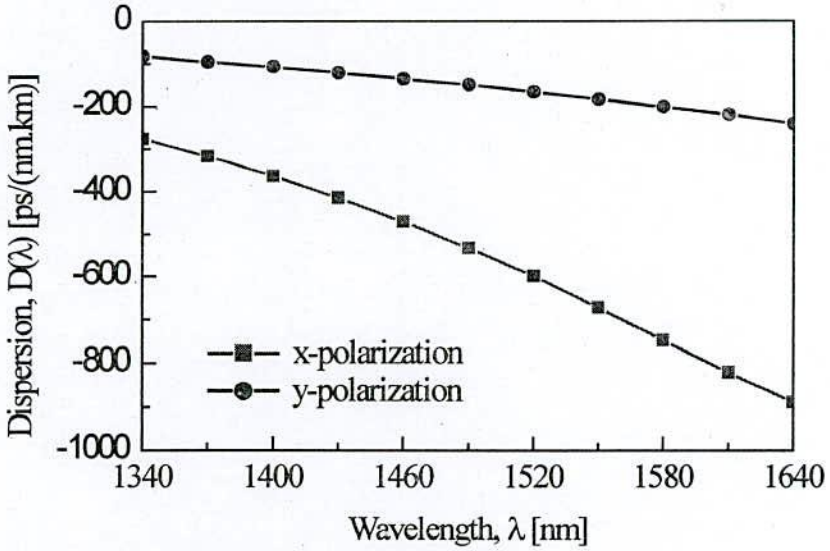

Fig. 4.42 Wavelength response of chromatic dispersion of the proposed M-OPCF for both x- and y-polarization for the optimum design parameters.

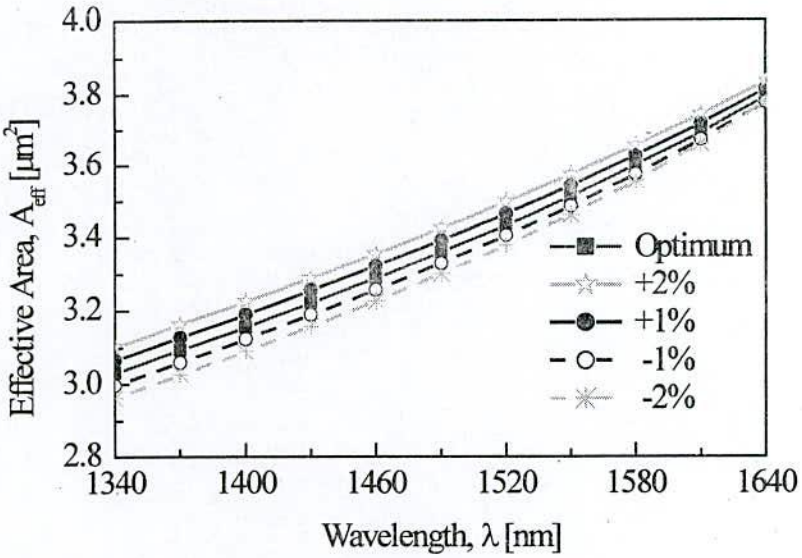

Fig. 4.43 Effective area of the proposed M-OPCF for optimum design parameters and also for fiber's global diameter variations of order ±1 to ±2% around the optimum value.

PCFs with PM properties are enviable in many applications [18]. However, conventional PM fibers show a modal birefringence of about 5×10^{-4}. Fig. 4.42 shows wavelength response of chromatic dispersion of the proposed M-OPCF for optimum design parameters. Optimizing the parameters η, Λ, d_1, d_2 and d_3 negative dispersion coefficient of −672.24 ps/(nm.km) and −183 ps/(nm.km) are obtained at 1550 nm for x-polarized and y-polarized mode respectively. A larger value of air-hole diameter, d_1 is chosen for better field confinement, while the air-hole diameter, d_2 is chosen smaller to shape the dispersion slope. Fig. 4.43 corresponds to variation of effective area for global diameter variations of order ±1 to ±2% along with the optimum design parameters. It can be clearly seen that effective area is 3.51 μm^2 at 1550 nm for the optimum design parameters. It changes about ±0.06 μm^2 for ±2% change in parameters. Therefore, it can be concluded that the tolerances of ±2% in the global diameter variations don't affect the performance of effective area. However, wavelength dependence of fiber's confinement loss for optimum design parameters and also for fiber's global diameter variations of order ±1 to ±2% has been shown in Fig. 4.44. Note that the loss is increasing smoothly with the wavelength and there is no evidence of abrupt change in leakage. In particular, confinement loss at 1550 nm is less than 10^{-4} dB/m considering five air-hole rings. It is also evident from Fig. 4.44 that changes in design parameters up to ±2% have an insignificant effect on the confinement losses. The effective V-parameter has been shown

in Fig. 4.45. It is obvious from the figure that the proposed M-OPCF will only support single mode rather multimode as $V_{eff} < \pi$ over the wavelength band ranging from 1340 to 1640 nm.

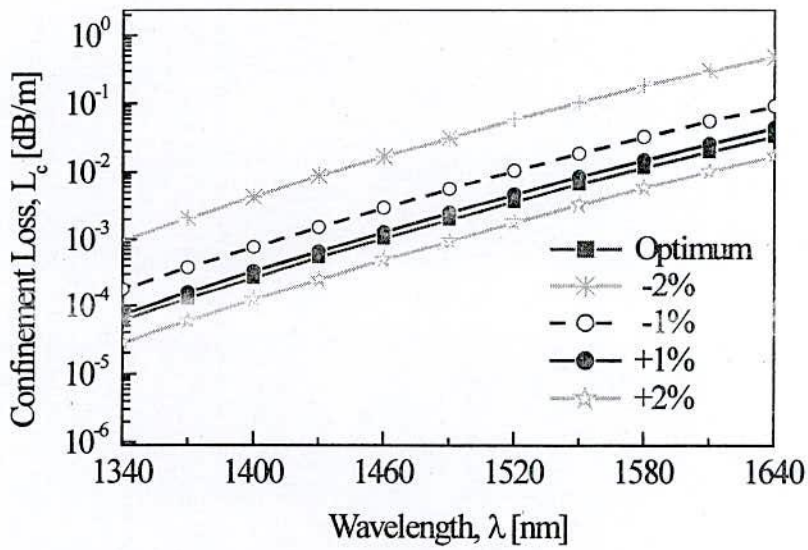

Fig. 4.44 Confinement loss of the proposed M-OPCF for the optimum parameters and also for fiber's global diameter variations of order ±1 to ±2% around the optimum value.

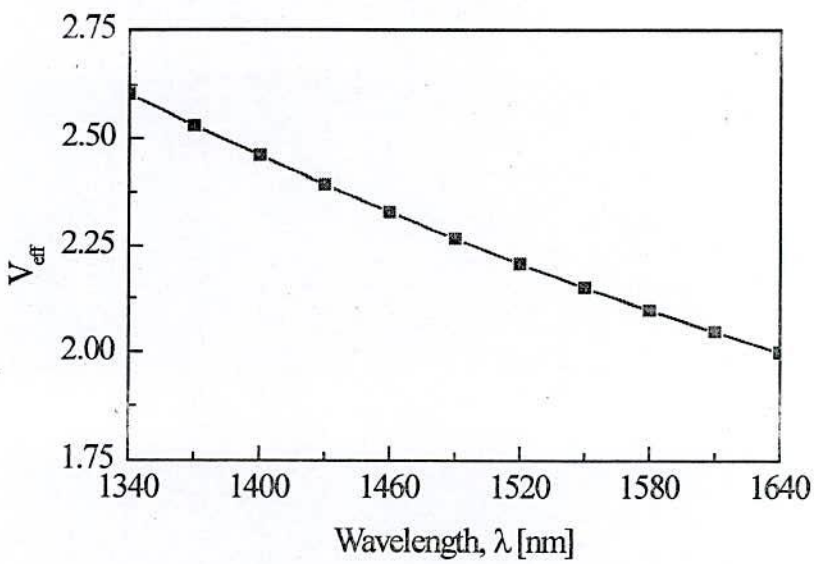

Fig. 4.45 Variation of effective V-parameter for the optimized M-OPCF.

4.5 Comparison between proposed DC-PCFs and some other DC-PCFs

Finally, a comparison is made between properties of the proposed PCFs for broadband dispersion compensation and some other PCFs designed for the same. The comparison between these fibers are presented in Table 2 which takes into account the magnitude of negative dispersion, birefringence, effective area, the length of dispersion compensating fiber to compensate the accumulated dispersion of the SMF and the number of design parameters (NDP). The magnitude of negative dispersion of the proposed DC-PCFs exhibit higher value that those presented. However, the C-PCF shows higher than that of other proposed DC-PCFs and hence it requires small length of DCF to compensate the accumulated dispersion of SMF but the birefringence is not enough. As a result, it will not be an appropriate candidate to compensate chromatic dispersion and PMD at the same time. On the other hand, M-CPCF and M-OPCF both show high birefringence in comparison with Ref. [2, 4, 16]. Moreover, the length required to compensate the accumulated dispersion of the SMF is less for the proposed designs than those presented in Table 2. In addition, the effective are of the M-OPCF is higher than that of Ref. [2, 4, 16].

Table 3: Comparison between properties of the proposed DC-PCFs and other DC-PCFs at 1550 nm wavelength

PCFs	Dispersion ps/(nm.km)	B ($\lvert n_x - n_y \rvert$)	A_{eff} (μm^2)	Length of DCF (km)	NDP (N_r, N_Λ, N_d)
C-PCF	-790.12	7×10^{-4}	1.65	0.82	5, 1, 4
M-CPCF	-643.62	2.2×10^{-2}	2.05	1.15	5, 1, 3
M-OPCF	-672.24	2.53×10^{-2}	3.51	1.10	5, 1, 3
Ref. [2]	-	-	1.55	-	5, 1, 1
Ref. [4]	-239.5	1.67×10^{-2}	2.60	2.27	6, 1, 1
Ref. [16]	-588	1.81×10^{-2}	3.43	1.17	5, 1, 2

However, the comparison between relative dispersion slopes of the proposed DC-PCFs has been shown in Fig. 4.46. It is observed that the relative dispersion slope of the proposed fibers is equal to the relative dispersion slope of SMF of about 0.0036 nm^{-1} at 1550 nm wavelength. The comparison between effective dispersion in Fig. 4.46 reveals that the M-CPCF is appropriate for dispersion compensation covering entire E to L band wavelength ranging from 1360 to 1625 nm as the effective dispersion is less than ±0.8 s/(nm.km) within that bands. In addition, there is a tendency to cover above the L band beyond 1640 nm wavelength.

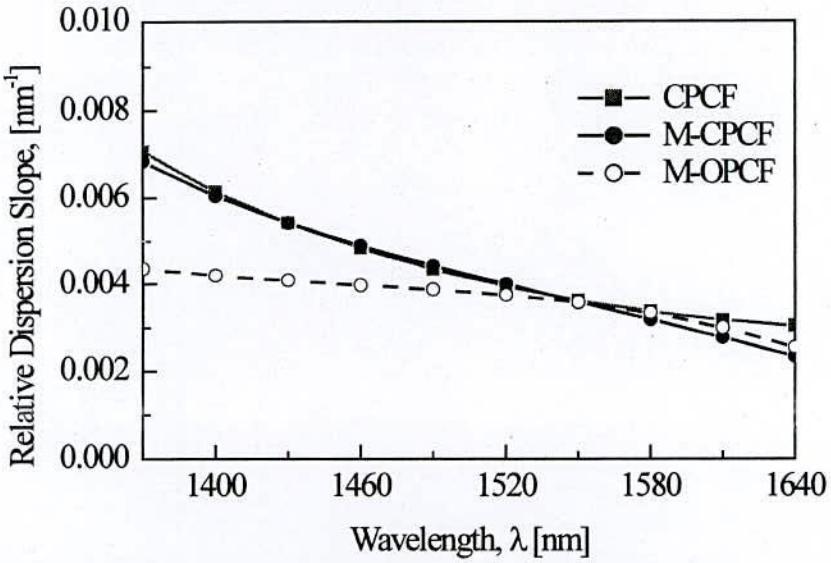

Fig. 4.46 Comparison between relative dispersion slope for the proposed DC-PCFs.

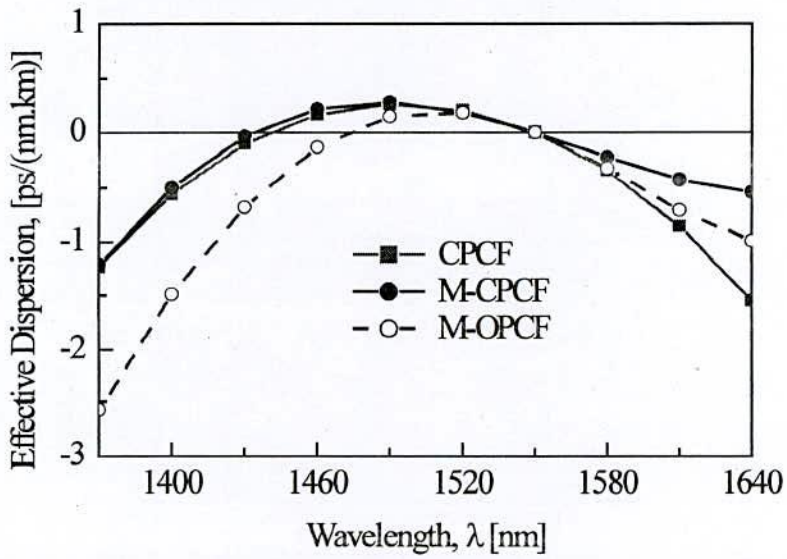

Fig. 4.47 Comparison between effective dispersion of the proposed DC-PCFs.

However, the M-OPCF is capable of compensating dispersion within S to L wavelength band whereas the C-PCF is able to compensate the dispersion of S and C band efficiently. However, it is expected that the proposed fiber will outperform than others. A comparison between confinement losses has been presented in Fig. 4.48. Confinement loss is lowest for M-OPCF compared to other designs.

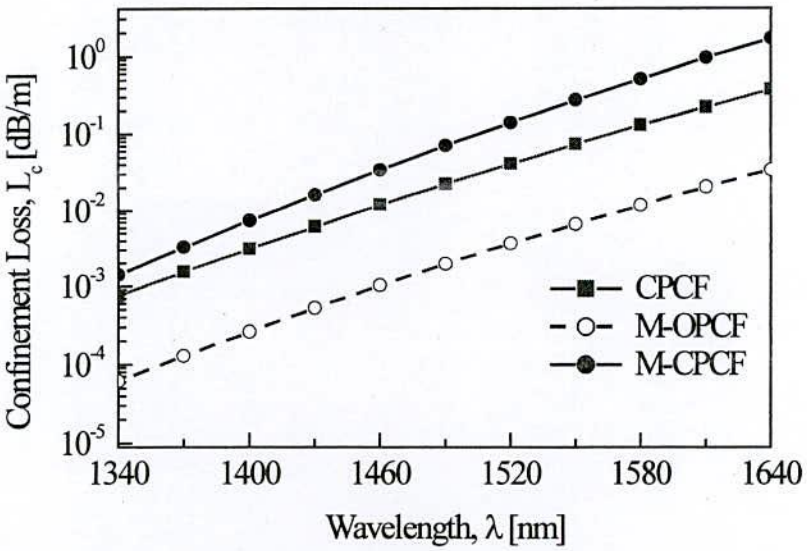

Fig. 4.48 Comparison between confinement losses of the proposed DC-PCFs.

4.6 Conclusion

Some designs of broadband DC-PCFs with high negative dispersion coefficient over a wide band of wavelength for effective dispersion compensation of SMF have been presented based on the FEM. According to numerical results the proposed designs provide high negative dispersion coefficient and an RDS matched with a conventional single mode fiber of about $0.0036nm^{-1}$. At the same time the proposed DC-PCFs ensure the effective dispersion within ±0.80 ps/(nm.km) which allow the designed fibers to be suitable for compensating 40Gbps covering E, S, C and L communication bands. The proposed DC-PCFs exhibit high birefringence of order 10^{-2} with the high negative dispersion characteristics which eliminate the effect of PMD along with chromatic dispersion. The characteristics of broadband dispersion compensation and high birefringence make the proposed fibers potential candidates as its application in the fiber optic communication link in the telecommunication window.

References

[1] F. Begum, Y. Namihira, S. M. A. Razzak, S. F. Kaijage, N. H. Hai, T. Kinjo, K. Miayagi, N. Zou, "Novel broadband dispersion compensating photonic crystal fibers: Applications in high speed transmission," *Optic and Laser Technology*, vol. 41, no. 6, pp. 679-686, Sep. 2009.

[2] M. Selim Habib, M. Samiul Habib, S. M. A. Razzak, Y. Namihira, M. A. Hossain, and M. A. G Khan, "Broadband dispersion compensation of conventional single mode fibers using microstructure optical fibers," *Optik-International Journal for Light and Electron Optics*, vol. 124, no. 19, pp. 3851–3855, Oct. 2013.

[3] F. Poli, A. Cucinotta, S. Selleri, and A. H. Bouk, "Tailoring of flattened dispersion in highly nonlinear photonic crystal fibers," *IEEE Photonics Technology Letters,* vol. 16, pp. 1065–1067, 2004.

[4] F. Kaijage, Y. Namihira, N. H. Hai, F. Begum, S. M. A. Razzak, T. Kinjo, K. Miayagi, and N. Zou, "Broadband dispersion compensating octagonal photonic crystal fiber for optical communication applications," *Japanese Journal of Applied Physics*, vol. 48, 2009.

[5] M. Selim Habib, M. Samiul Habib, S. M. A. Razzak, Y. Namihira, M. A. Hossain, and M. A. G Khan, "Broadband dispersion compensation of conventional single mode fibers using microstructure optical fibers," *Optik-International Journal for Light and Electron Optics*, vol. 124, no. 19, pp. 3851–3855, Oct. 2013.

[6] R. R. Musin, and A. M. Zheltikov, "Designing dispersion-compensating photonic-crystal fibers using a genetic algorithm," *Optical Communication*, vol. 281, no. 4, pp. 567-572, Feb. 2008.

[7] M. Koshiba, and K. Saitoh, "Structural dependence of effective area and mode field diameter for holey fibers," *Optics Express*, vol. 11, no. 15, pp. 1746–1756, Jul. 2003.

[8] S. G. Leon-Saval, T. A. Birks, N. Y. Joy, A. K. George, W. J. Wadsworth, G. Kakarantzas, and P. St. J. Rusell, "Splice-free interfacing of photonic crystal fibers," *Optics Letters*, vol. 30, pp. 1629-1631, 2005.

[9] T. Fujisawa, K. Saitoh, K. Wada, and M. Koshiba, "Chromatic dispersion profile optimization of dual concentric core photonic crystal fibers for broadband dispersion compensation," *Optics Express*, vol. 14, no. 2, pp. 893-900, Jan. 2006.

[10] Z. Xingtao, Z. Guiyao, L. Shuguang, L. Zhaolun, W. Dongbin, and H. Zhiyun, "Photonic crystal fiber for dispersion compensation," *Applied Optics*, vol. 47, no. 28, pp. 5190-5196, Oct. 2008.

[11] S. K. Varshney, T. Fujisawa, K. Saitoh, and M. Koshiba, "Design and analysis of a broadband dispersion compensating photonic crystal fiber Raman amplifier operating in S-band," *Optics Express*, vol. 14, no. 8, pp. 3528-3540, Apr. 2006.

[12] P. J. Roberts, B. J. Mangan, H. Sabert, F. Couny, T. A. Birks, J. C. Knight, and P. St. J. Russell, "Control of dispersion in photonic crystal fibers," *Journal of Optical Fiber Communication Report*, vol. 2 pp. 435-461, 2005.

[13] W. H. Reeves, J. C. Knight, and P. S. J. Russell, "Demonstration of ultra-flattened dispersion in photonic crystal fibers," *Optic Express*, vol. 10, no.14pp. 609–613, 2002.

[14] F. Poletti, V. Finazzi, T. M. Monro, N. G. R. Broderick, V. Tse, and D. J. Richardson, "Inverse design and fabrication tolerances of ultraflattened dispersion holey fibers," *Optics Express*, vol. 13, no. 10, pp. 3728–3736, 2005.

[15] S. M. A. Razzak, and Y. Namihira, "Highly birefringent photonic crystal fibers with near-zero dispersion at 1550 nm wavelength," *Journal of Modern Optics*, vol. 56, pp. 1188-1193, 2009.

[16] M. Selim Habib, M. Samiul Habib, and S. M. A. Razzak, "Proposal for Highly Birefringent Broadband Dispersion Compensating Octagonal Photonic Crystal Fiber," *Optical Fiber Technology*, vol. 19, no. 5, pp. 461–467, Oct. 2013.

[17] S. Kim,C. Kee, and C. G. Lee, "Modified rectangular lattice photonic crystal fibers with high birefringence and negative dispersion," *Optics Express*, vol. 17, pp. 7952-7957, 2009.

[18] G. P. Agrawal, "Fiber-optic Communication Systems," 3rd edition, Chapter 7, Wiley, New York, 2002.

[19] M. M. Haque, M. S. Rahman, M. Samiul Habib, M. Selim Habib, and S. M. A. Razzak, "A new circular photonic crystal fiber for effective dispersion compensation over E to L wavelength bands," *Journal of Microwaves, Optoelectronics and Electromagnetic Applications,* vol. 12, no. 2, pp. 44-54, 2013.

[20] M. Selim Habib, M. Mejbaul Haque, M. Samiul Habib, M. I. Hasan, M. Shaifur Rahman, and S. M. A. Razzak, "Polarization maintaining holey fibers for residual dispersion compensation over S + C + L wavelength bands," *Optik - International Journal for Light and Electron Optics*, vol. 125, no. 3, pp. 911-915, 2014.

CHAPTER V

Conclusions and Suggestions

5.1 Conclusion

In this thesis, following research aspects have been reported: (1) modeling of broadband DC-PCFs for effective dispersion compensation of SMF including C-PCF, M-CPCF and M-OPCF using COMSOL Multiphysics 4.2 which is based on FEM, (2) requirement of the broadband dispersion compensation, (3) investigation of high negative dispersion phenomenon in the designed DC-PCFs that is needed to compensate the positive dispersion of the SMF during transmission of signals, (4) investigation of the dispersion accuracy of the proposed designs using global diameter variation and individual design parameter variation (5) investigation of the RDS value which is required to be exactly equal to 0.0036 nm^{-1} at 1550 nm wavelength and the dispersion slope needed to be negative for broadband dispersion compensation of SMF, (6) effective dispersion to judge the dispersion compensation capability of the proposed DC-PCFs, (7) analysis of high birefringence properties of the proposed fibers to eliminate the effect of PMD, (8) analysis of effective area and hence its potential difficulties in the input coupling and output coupling of light, (9) investigation of the confinement loss of the proposed designs and the length required to compensate the accumulated dispersion of SMF, (10) investigation of the number of modes supported by the proposed DC-PCFs. The effective refractive index, n_{eff} of the fundamental mode was found by numerical simulation of the proposed DC-PCFs using COMSOL Multiphysics 4.2. Subsequently properties mentioned above were determined using some computations presented in section 3.4. However, the proposed C-PCF showed a high negative dispersion of about -790 ps/(nm.km) at 1550 nm and the dispersion slope was also negative for the optimum design parameters. Moreover, the residual dispersion slope was equal to the residual dispersion slope of SMF of about 0.0036 nm^{-1} at 1550 nm wavelength. Although, it experienced a drastic change in dispersion when pitch, Λ is varied up to ± 2%, the effective dispersion was within ± 0.8 ps/(nm.km) over the wavelength ranging from 1400 to 1610 nm. Hence, C-PCF could be applicable for broadband dispersion compensation in a high bit rate transmission systems especially in the S to L communication band. However, the effective area was small and in particular, at 1550 nm the value of effective area was 1.65 μm^2. In addition, the

confinement loss was within permissible limit and was further decreased with increasing the number of air hole rings. It is noteworthy that the birefringence of the proposed fiber was not enough and thus unable to eradicate the effect of PMD. With the aim of improving the birefringence, the C-PCF has been modified by breaking the symmetry between fiber axes introducing axial artificial defects. Hence, it was named M-CPCF. However, the M-CPCF showed a high negative dispersion of about -643.62 ps/(nm.km) with high birefringence of about 2.2×10^{-2} at 1550 nm wavelength. The chance in dispersion due to the fiber's structural parameter variation and also for fiber's global diameter variation was found consistent. Additionally, the RDS was perfectly matched with the RDS of SMF and the dispersion slope was found negative with a lower variation. The effective dispersion of the M-CPCF was found within ± 0.8 ps/(nm.km) over the wavelength ranging from 1400 to 1640 nm. Thus, the proposed M-CPCF should be applied for broadband dispersion compensation of SMF. The effective area was also increased significantly in comparison with C-PCF and it was 2.05 at 1550nm wavelength. Nevertheless, the confinement loss for the proposed M-CPCF is higher than that of other designs. Finally, the M-OPCF has been further presented to achieve better results than that of two fibers. However, it demonstrated a higher value of negative dispersion and birefringence of about -672.24 ps/(nm.km) and 2.53×10^{-2} respectively at 1550 nm wavelength compared to M-CPCF. The dispersion accuracy was also consistent because the dispersion was not changed drastically with the fiber's structural parameter variation. The effective area for M-OPCF was found higher compared to other two proposed fibers. Nevertheless, the effective dispersion was found within ± 0.8 ps/(nm.km) over the wavelength ranging from 1430 to 1610 nm. So, the available bandwidth for dispersion compensation was noticed 180 nm which was 60 nm and 30 nm less than that of M-CPCF and C-PCF respectively. The number of modes supported by the proposed DC-PCFs has been checked with the help of effective V-parameter. However, effective V-parameter V_{eff} was found less than 3.1416 for all three proposed DC-PCFs. Thus, the proposed fiber would have only support single mode and hence no multimode dispersion will be incurred during the operation as broadband DCF. It should also be mentioned that the proposed fiber except C-PCF would be suitable for a number of future application such as PM devices and sensing system due to its high birefringence.

5.2 Suggestions for future works

In this work, some designs of DC-PCFs have been demonstrated and then, performance of the proposed DC-PCFs have been presented and discussed. However, the proposed DC-PCFs show better dispersion compensating ability for compensating the dispersion of the SMF. Nevertheless, some limitations are still with the proposed designs that should be improved to enhance the performance of the proposed DC-PCFs. For example, the effective area of the proposed fibers is small which presents potential difficulties in the input coupling and output coupling of light. Thus, efforts should be given to enrich the effective area of the fibers. Another major challenge is to make lower the confinement losses which are unavoidable of PCFs. Although the proposed DC-PCFs exhibit permissible confinement losses, some steps can further be taken to reduce the confinement losses. To reduce the complexity during fabrication process of the fibers, structural parameter should be minimum. However, proposed C-PCF has four different sized air hole diameters. In contrast, M-OPCF and M-CPCF has three different sized air hole diameters. Thus, the fabrication difficulties of the later designs are obviously lower that the former one. So, efforts should be given to reduce the number of structural parameters.

List of Publication

[1] **M. M. Haque**, M. S. Rahman, M. Samiul Habib, M. Selim Habib, and S. M. A. Razzak, "A new circular photonic crystal fiber for effective dispersion compensation over E to L wavelength bands," *Journal of Microwaves, Optoelectronics and Electromagnetic Applications,* vol. 12, no. 2, pp. 44-54, Dec. 2013.

[2] M. Selim Habib, **M. Mejbaul Haque**, M. Samiul Habib, M. I. Hasan, M. Shaifur Rahman, and S. M. A. Razzak, "Polarization maintaining holey fibers for residual dispersion compensation over S + C + L wavelength bands," *Optik - International Journal for Light and Electron Optics*, vol. 125, no. 3, pp. 911-915, Feb. 2014.